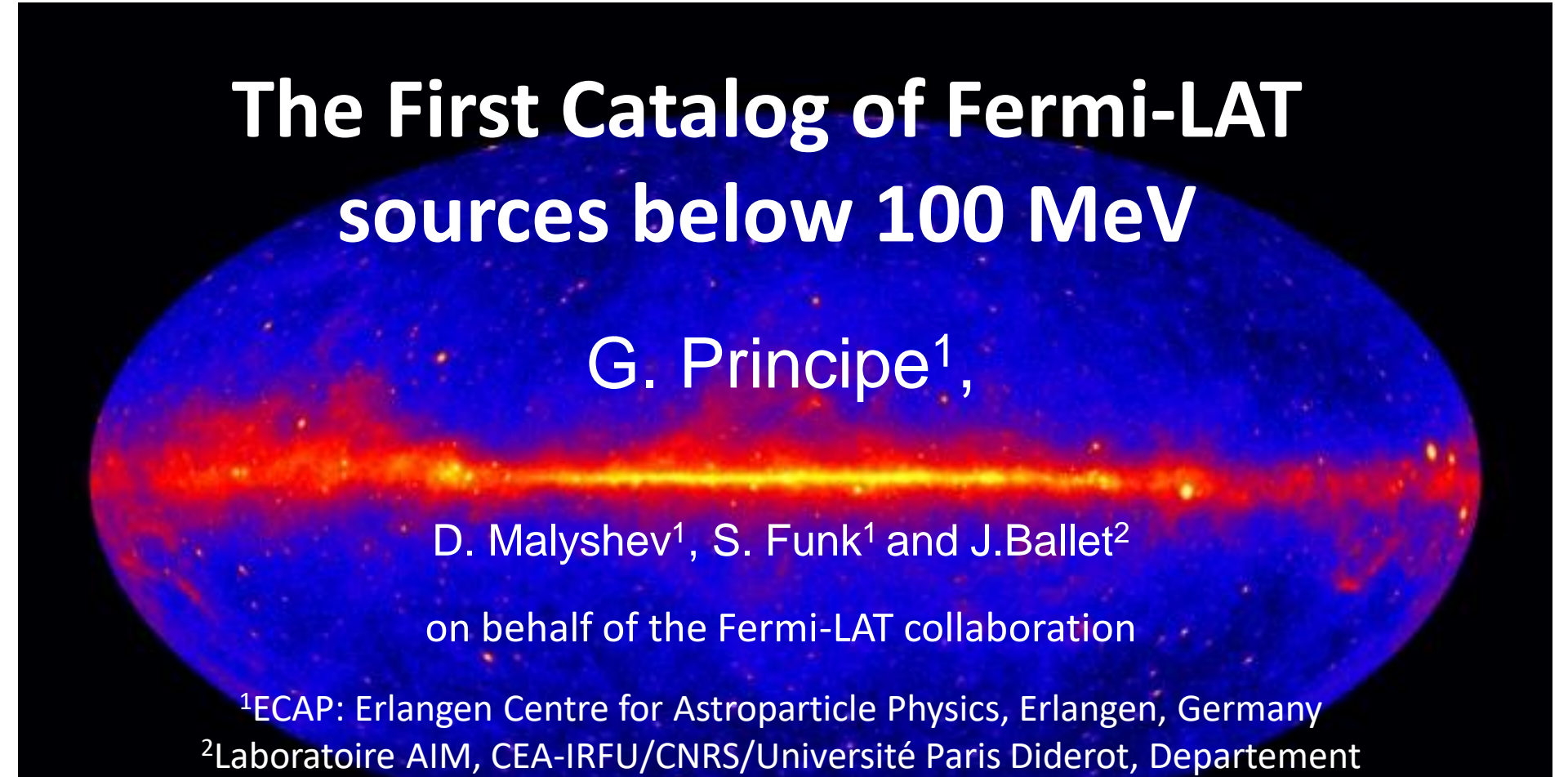


The First Catalog of Fermi-LAT sources below 100 MeV



G. Principe¹,

D. Malyshev¹, S. Funk¹ and J. Ballet²

on behalf of the Fermi-LAT collaboration

¹ECAP: Erlangen Centre for Astroparticle Physics, Erlangen, Germany

²Laboratoire AIM, CEA-IRFU/CNRS/Université Paris Diderot, Département d'Astrophysique, CEA Saclay, Gif sur Yvette, France

Content

The First Catalog of Fermi-LAT sources below 100 MeV (1FLE)

1. Introduction about Fermi-LAT and motivation of 1FLE

1. MC analysis

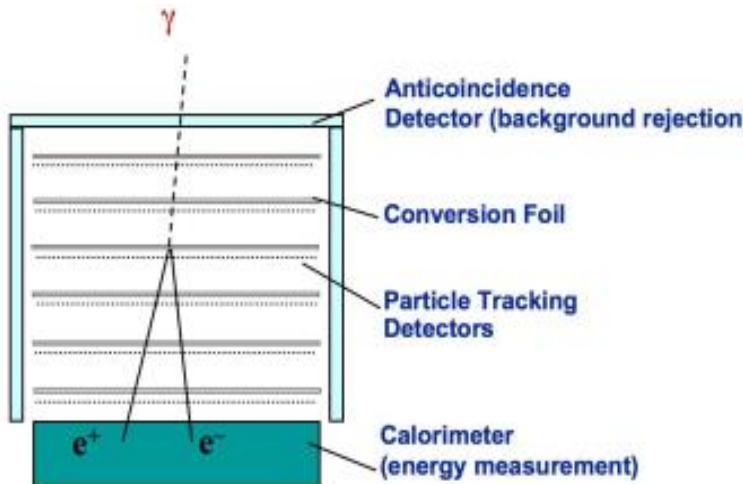
1. Data selection
2. PGWave parameter optimization
3. Flux reconstruction

3. Results

1. Comparison with the 3FGL catalog
2. 1FLE blazars
3. Sensitivity 1FLE

4. Summary

Fermi-LAT Instrument

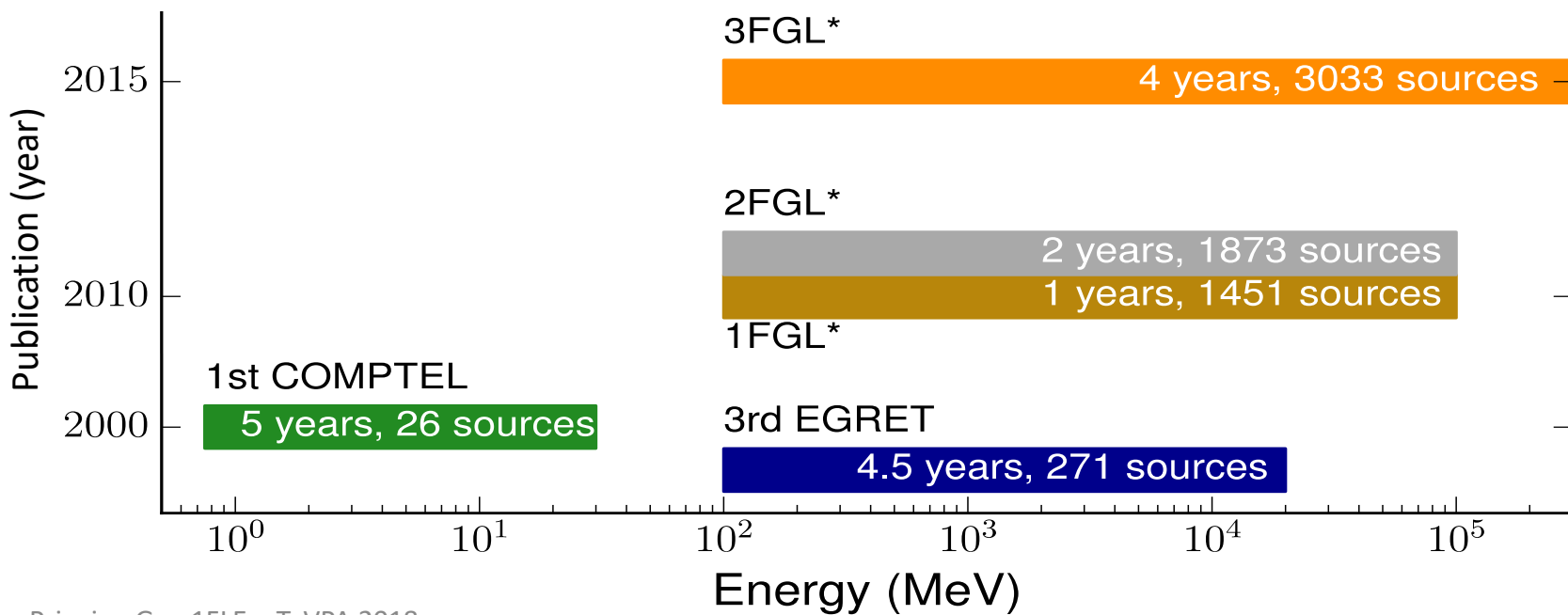


Fermi-LAT

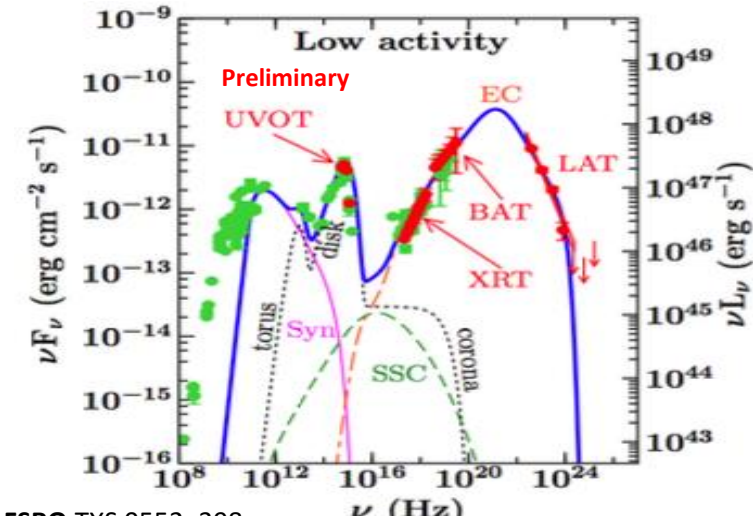
- Launch date: June 11, 2008
- Energy range: 20 MeV – 300 GeV
- General catalogs(*): 1FGL, 2FGL, 3FGL

[W. B. Atwood et al., Astrophys. Journ. 697 \(2009\), p. 1071.](#)

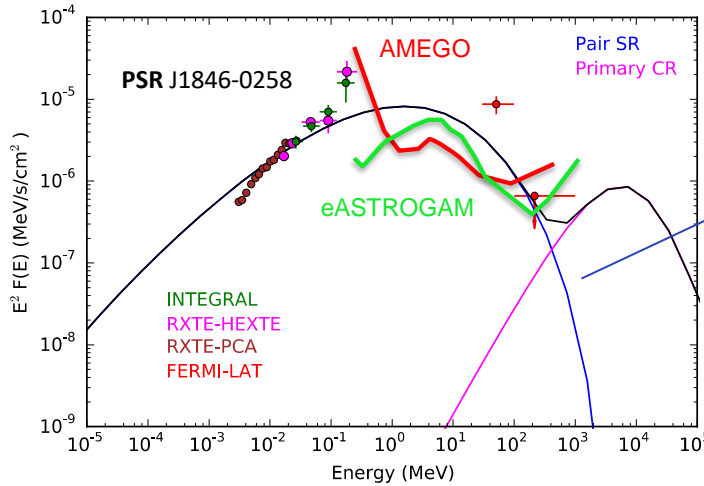
No catalogs between 30 and 100 MeV!



Missing MeV Sources?

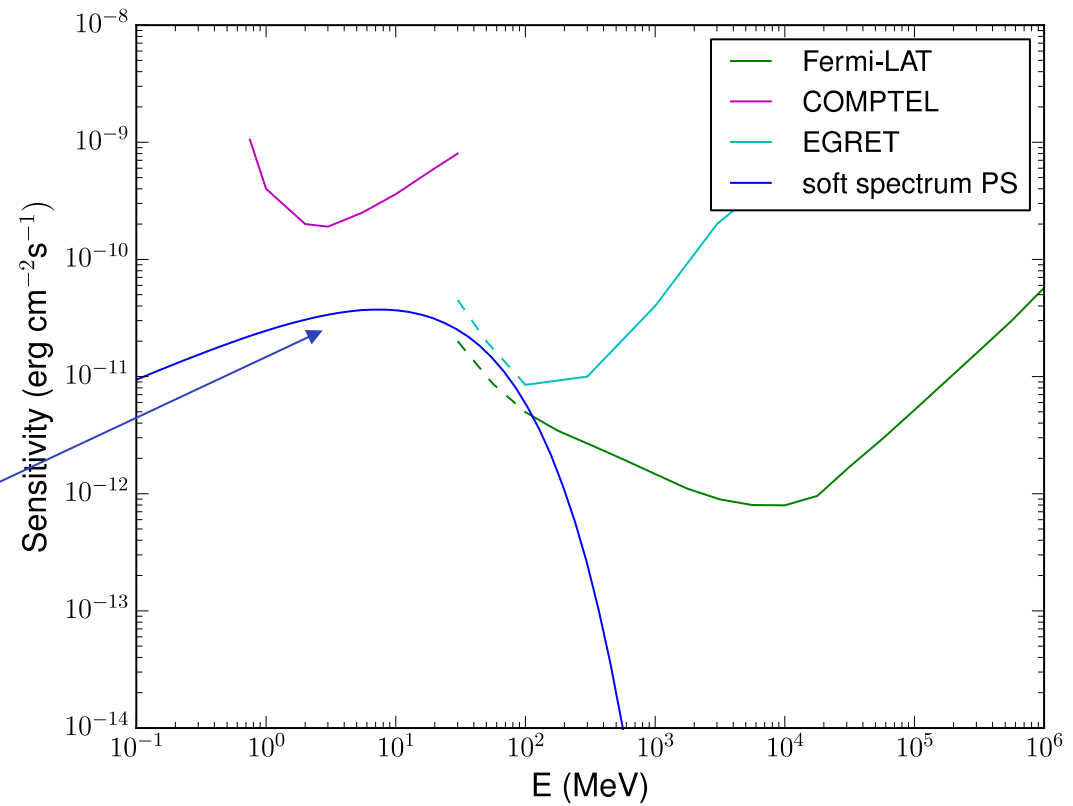


FSRQ TXS 0552+398
Vaidehi et. al. in prep.



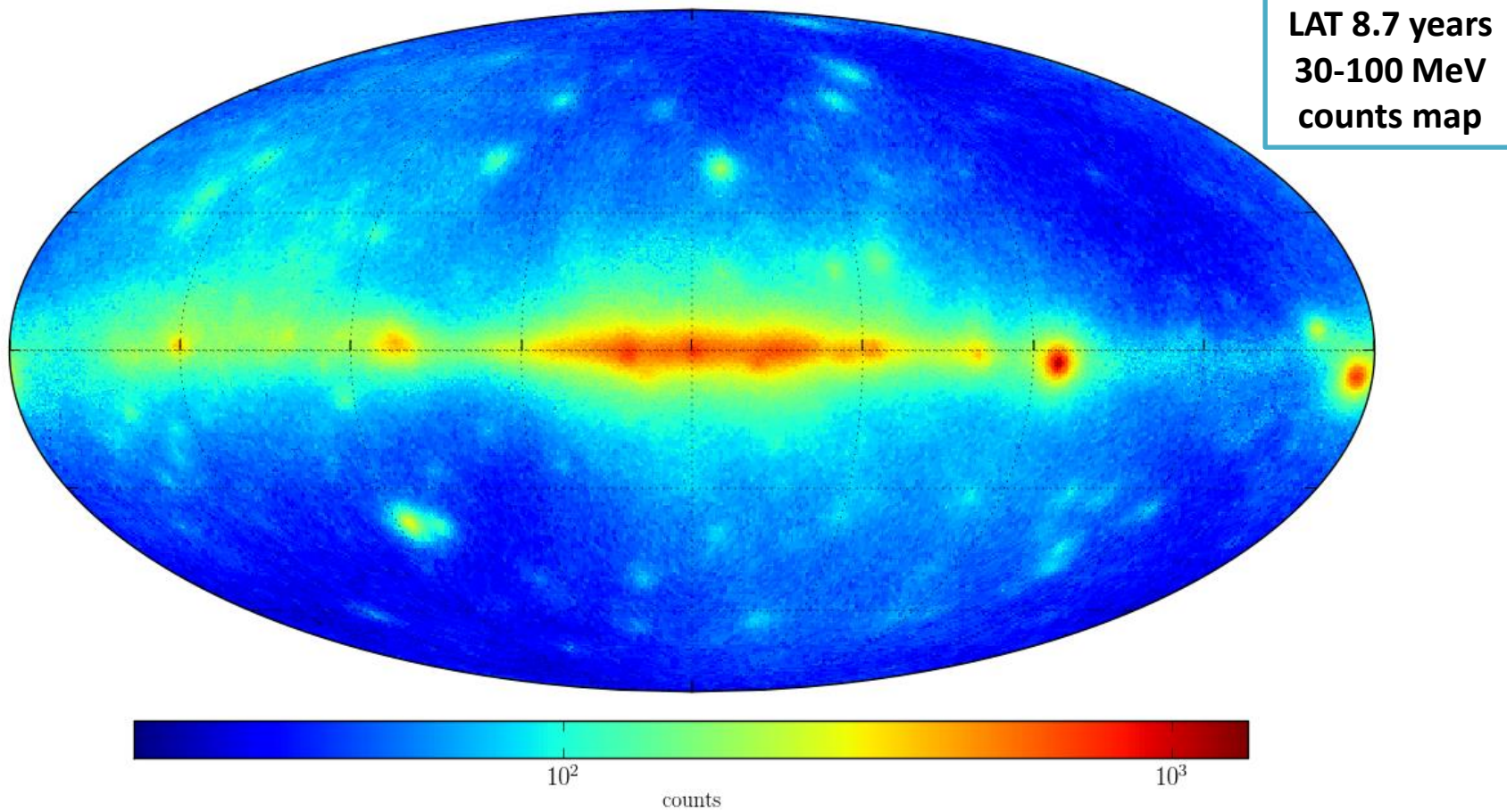
Harding et. al.(2017)

There exists a population of very energetic sources having hard X-ray emission but have no detected emission by Fermi LAT.



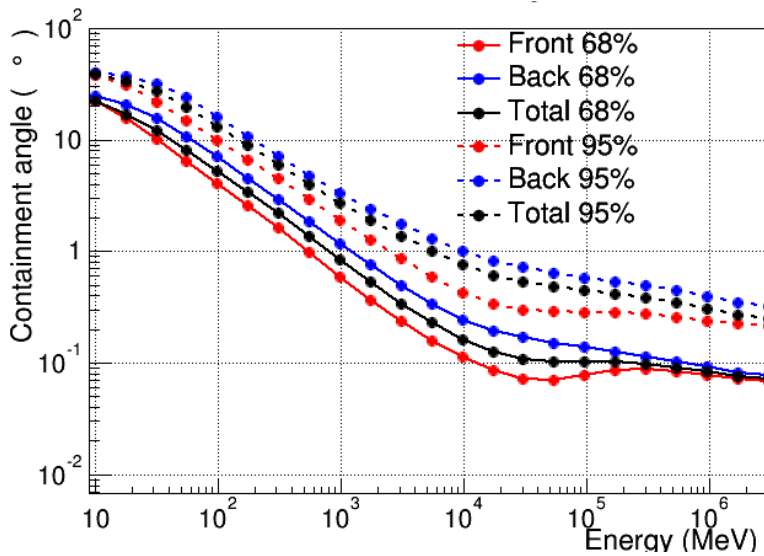
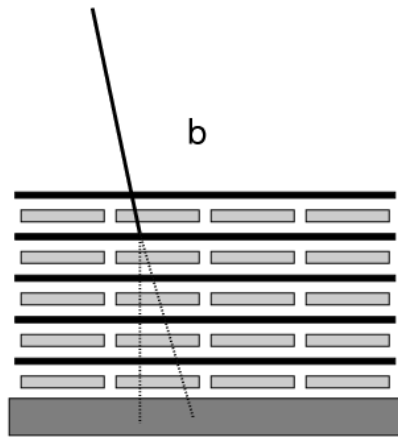
Fermi Low Energy Catalog

We are interested in studying the Fermi-LAT data between **30 and 100 MeV** since they were not covered in the previous Fermi-LAT Catalogs. To detect the sources and estimate their flux we want to use PGWave, a **background-independent method** already used in the Fermi-LAT catalog pipeline to find candidate sources.

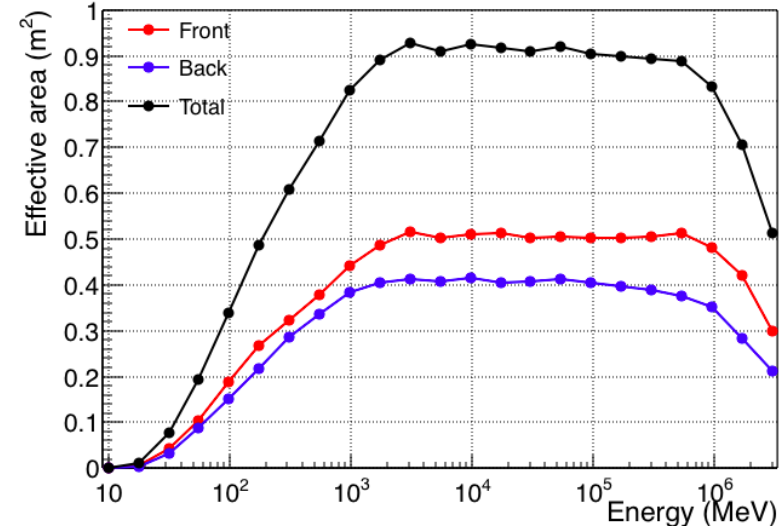
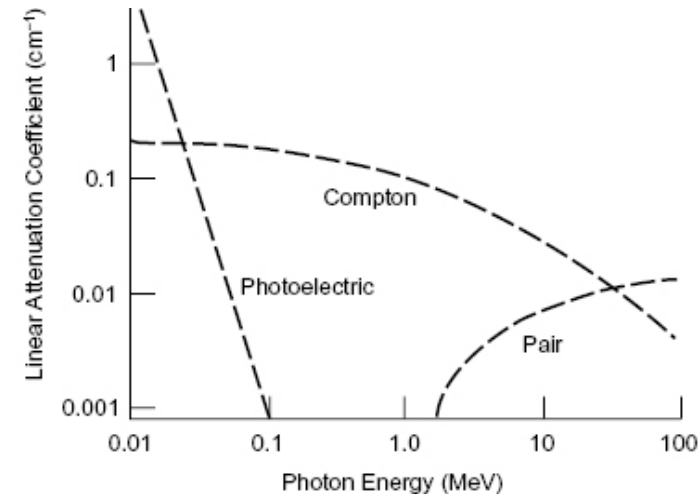


Why are there no Catalogs in the 30-100 MeV band?

1) Angular resolution gets worse



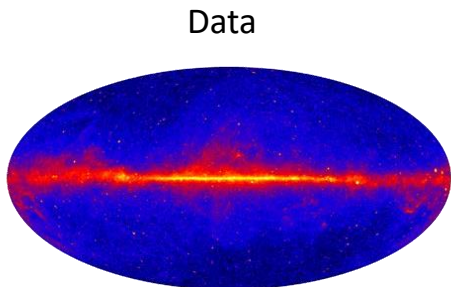
2) Effective area gets smaller



Gamma Sky Components

3) Difficulty in creating an accurate model for the diffuse emission

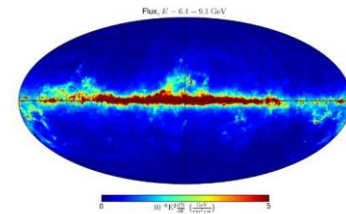
Galactic diffuse emission



Data

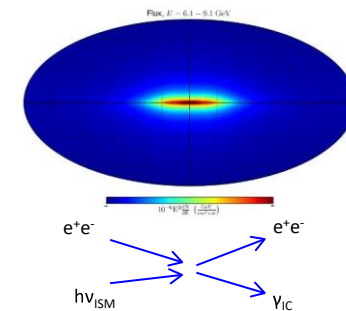
=

π^0 and bremsstrahlung



+

Inverse Compton

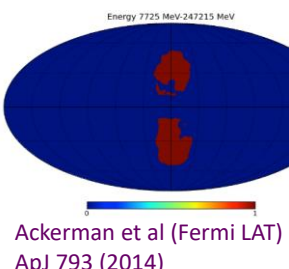


+

Isotropic
Extragalactic +
residual CR background

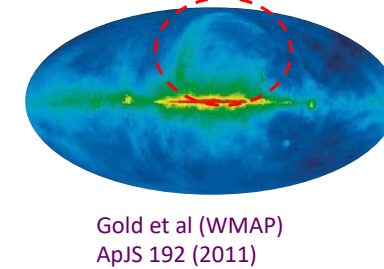
+

Bubbles



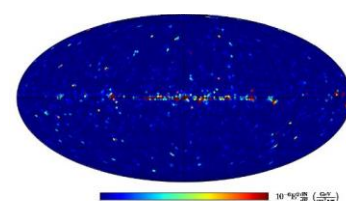
Ackerman et al (Fermi LAT)
ApJ 793 (2014)

Loop I



Gold et al (WMAP)
ApJS 192 (2011)

Point sources

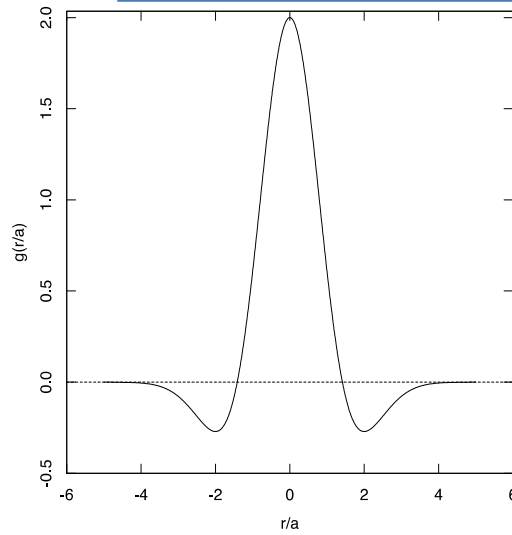


Fermi catalogs

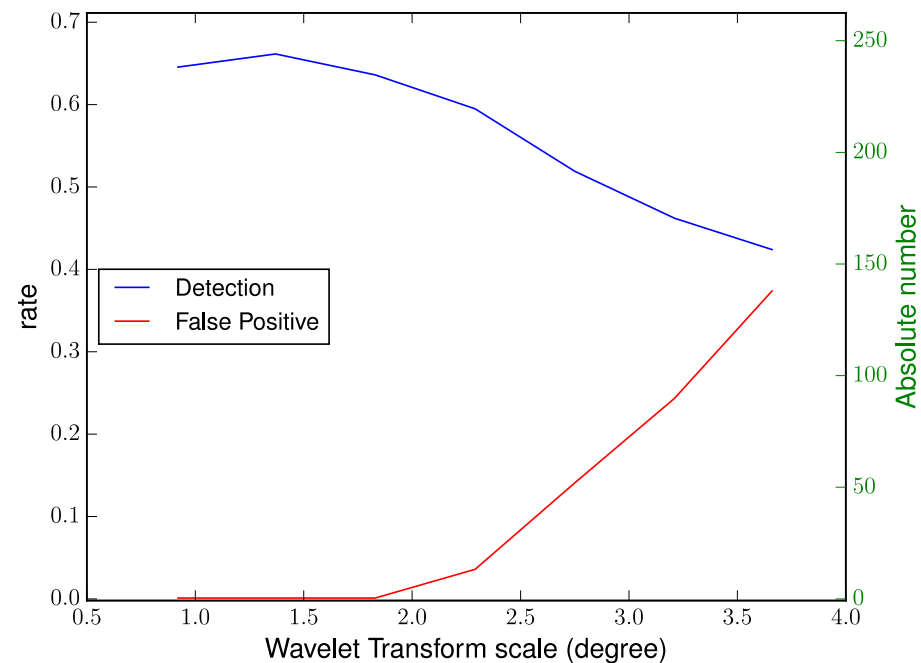
These reasons make the 30-100 MeV band one of the most complicated energy range!



PGWave Parameter optimization



PGWave uses the 2-dim “Mexican Hat” wavelet. (Damiani *et.al.* 1997)

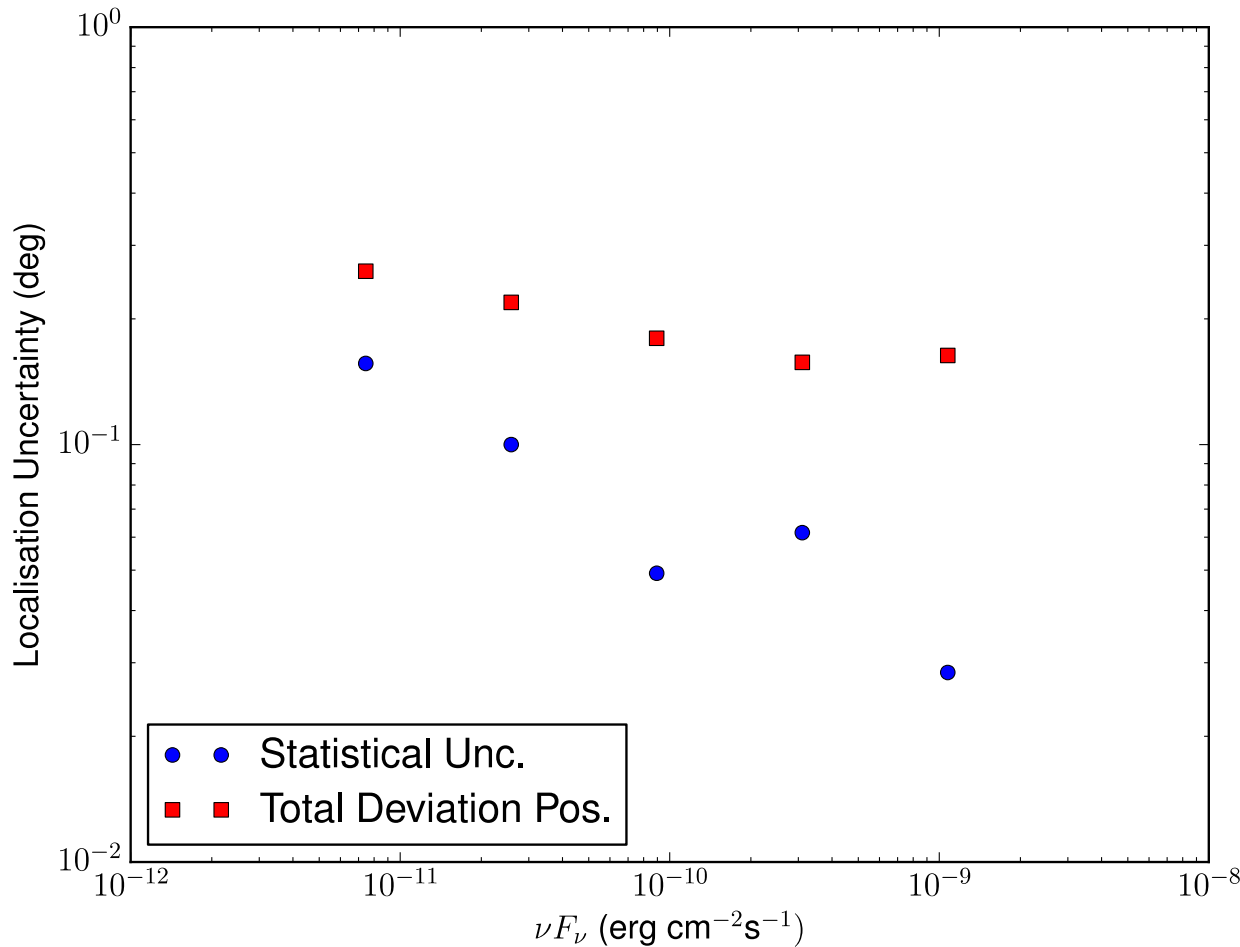


| PGWave parameters | 30 – 100 MeV | 100 – 300 MeV |
|-----------------------------------|--------------|---------------|
| Pixel dim. | 0°.458 | 0°.458 |
| N° sigma for the stat. confidence | 3 | 3 |
| MH Wavelet Transform scale | 1°.4 – 1°.8 | 0°.9 - 1°.8 |
| Min. number of connected pixels | 5 - 6 | 7 - 6 |
| Min. distance between sources | 1°.8 – 2°.7 | 1°.8 - 2°.7 |

False Positives:

- 5 in 30-100 MeV
- 17 in 100-300 MeV

Syst. and Stat. Uncertainty of PS Localization



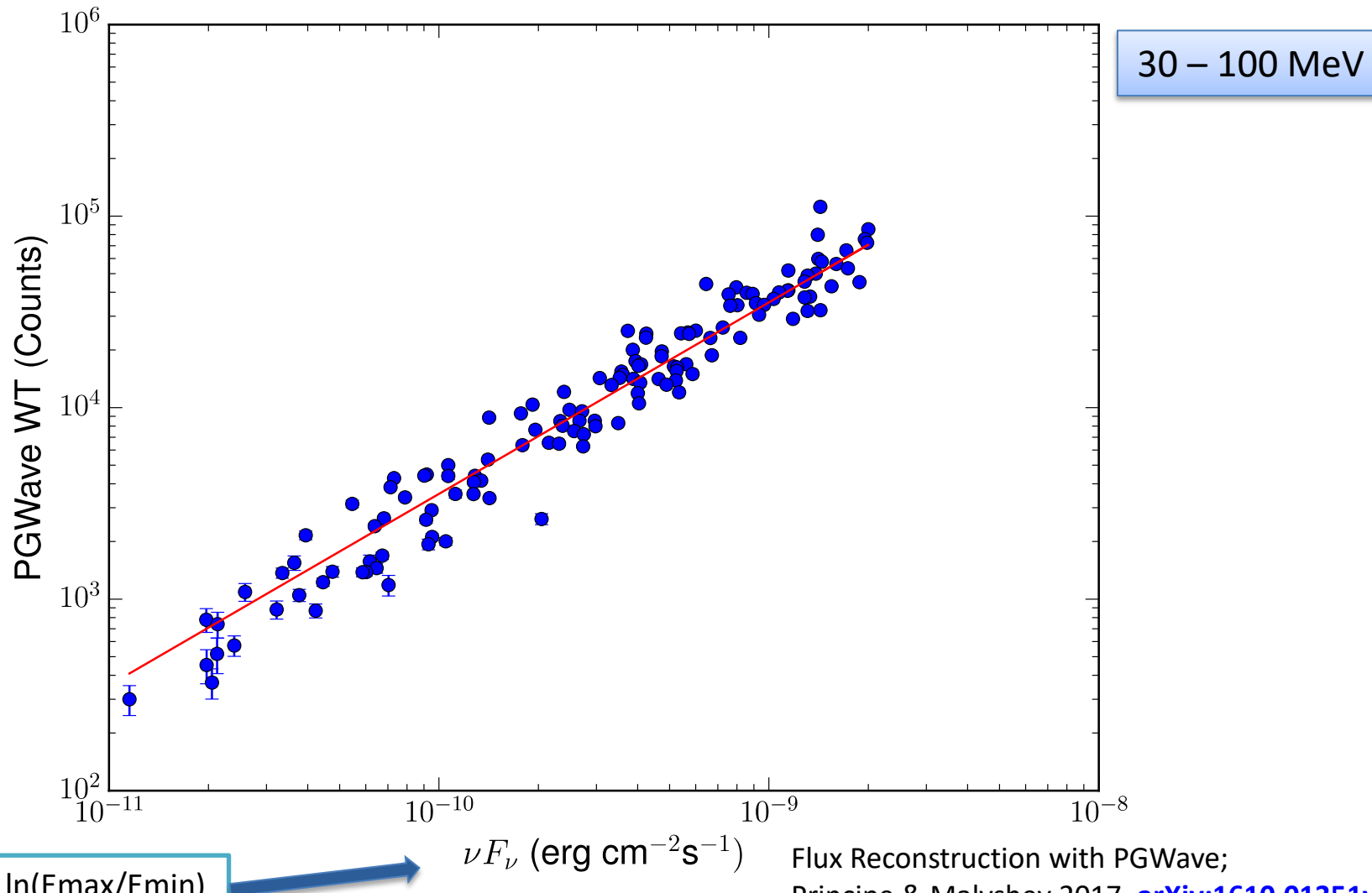
Using 10 realizations
Random PS maps

30 -100 MeV

Syst. Unc $\approx 0^\circ.25$

We optimize the position given by PGWave using a parabolic fit in 5x5 pixel grid around the maximum.

Flux Determination



Fermi-LAT sources below 100 MeV

Association:

- Based on a positional coincidence
- Tolerance radius 1.5°
- Flux ordering

Results

3FGL (grey points)

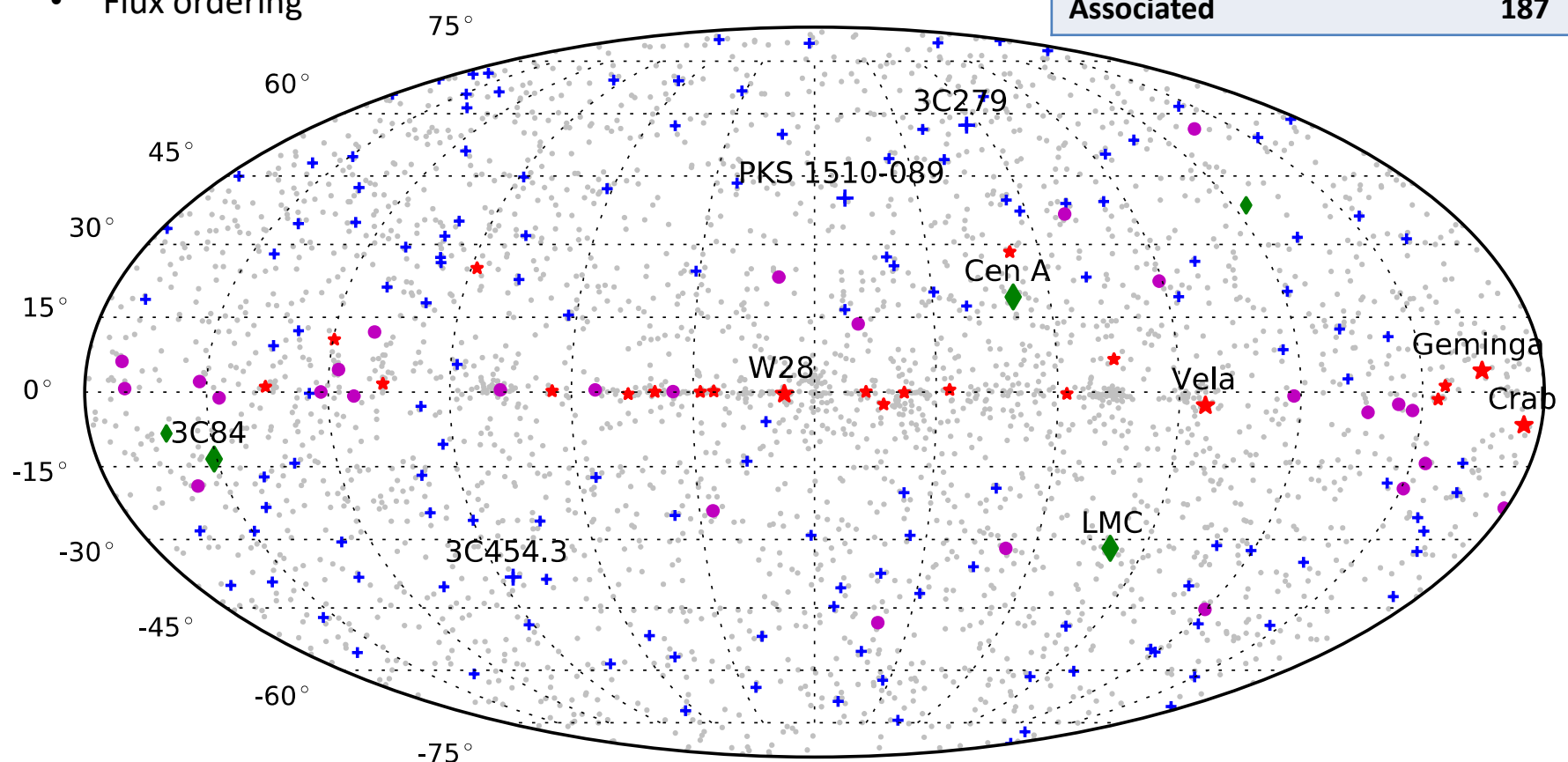
3034

PGWave 30-100 MeV

198

Associated

187



★ ★ ★ Pulsar, PWN, SNR, HMB

◆ ◆ ◆ Other Extragalactic Obj.

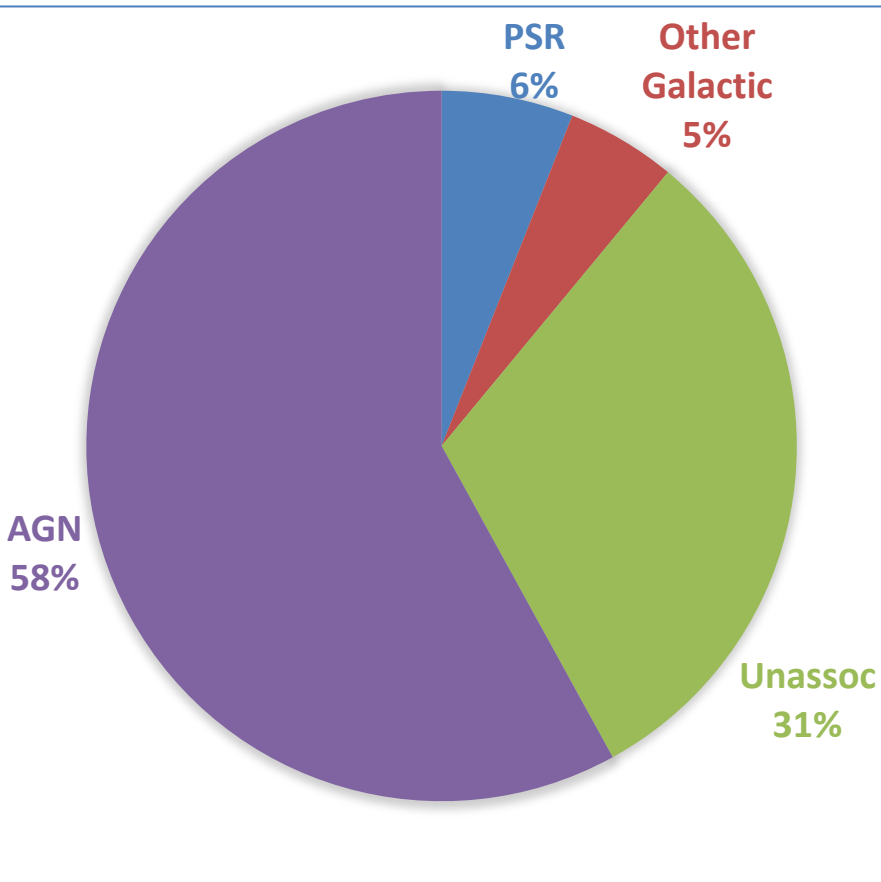
+ + + Blazar

● ● ● Unclassified or Unassociated

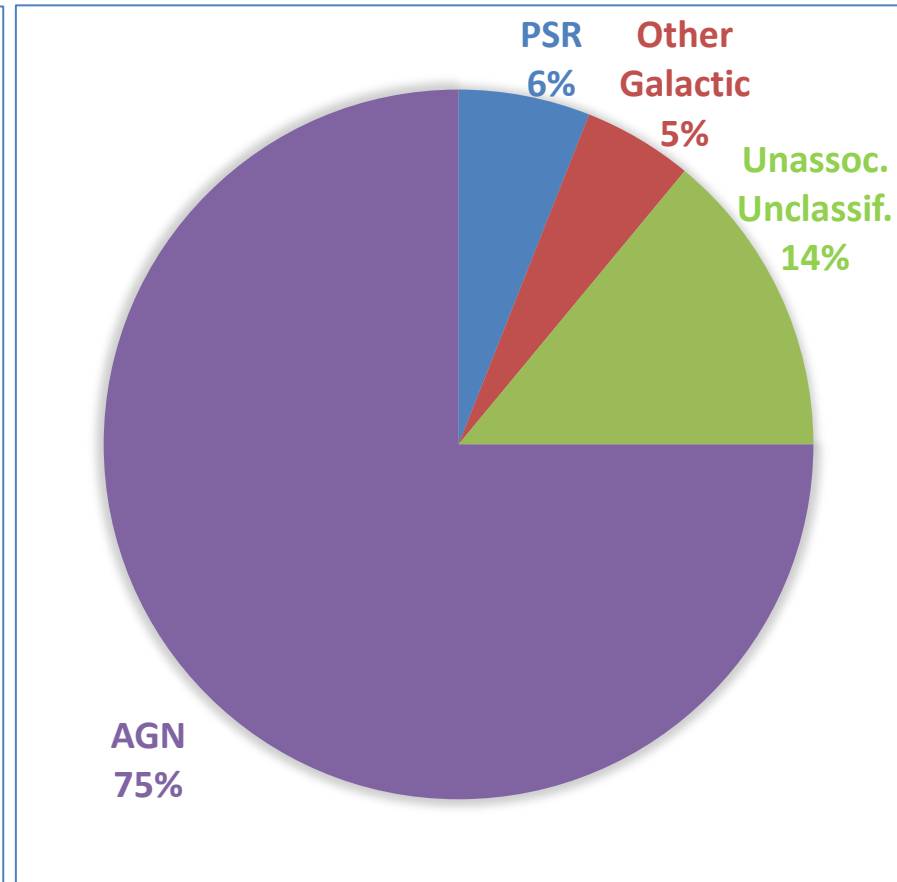
1FLE and 3FGL Catalog comparison

3FGL

(3033 sources)

**1FLE**

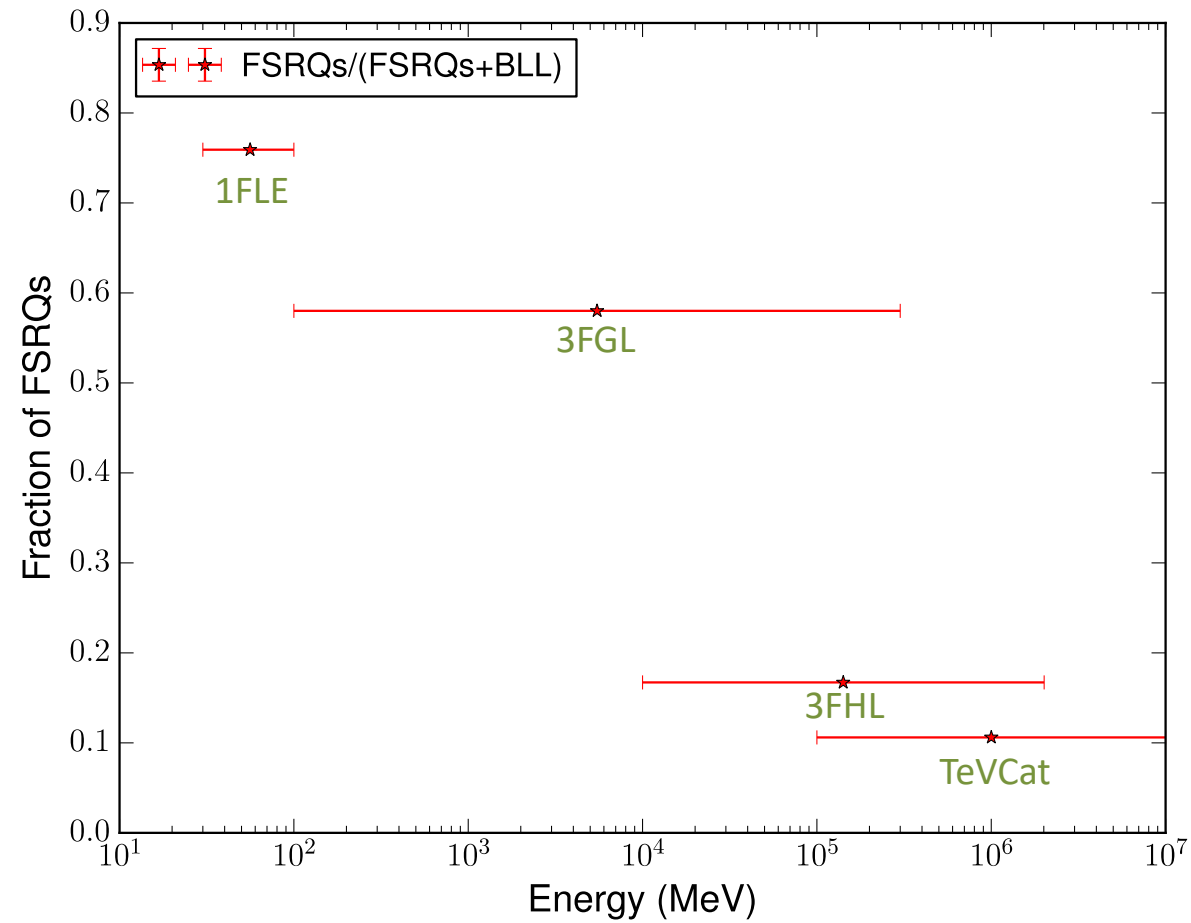
(198 sources)



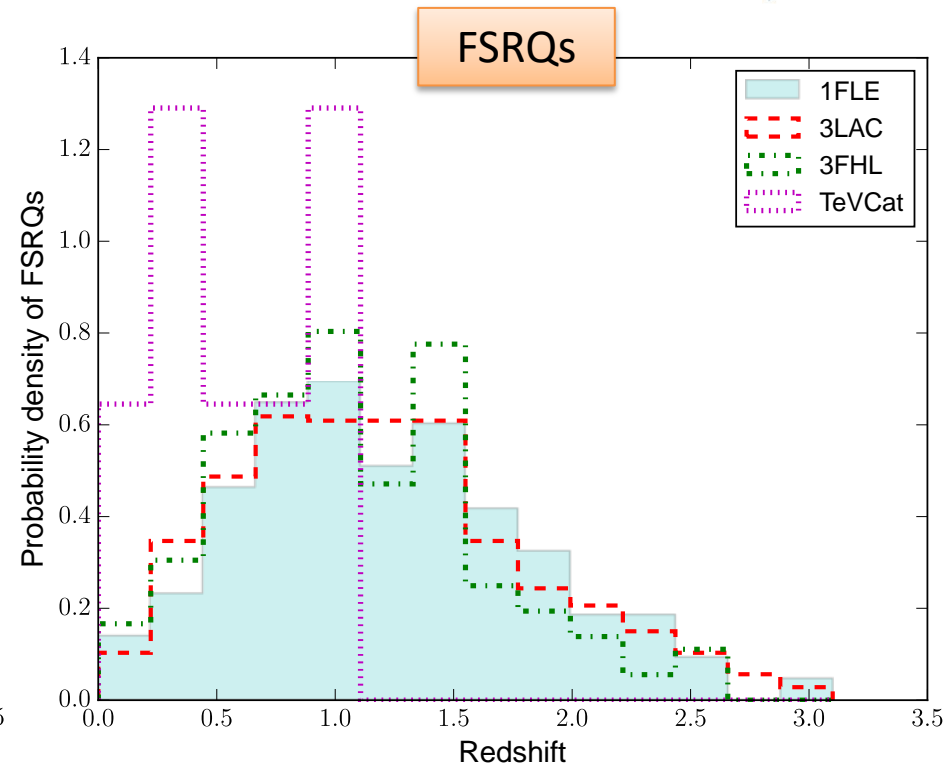
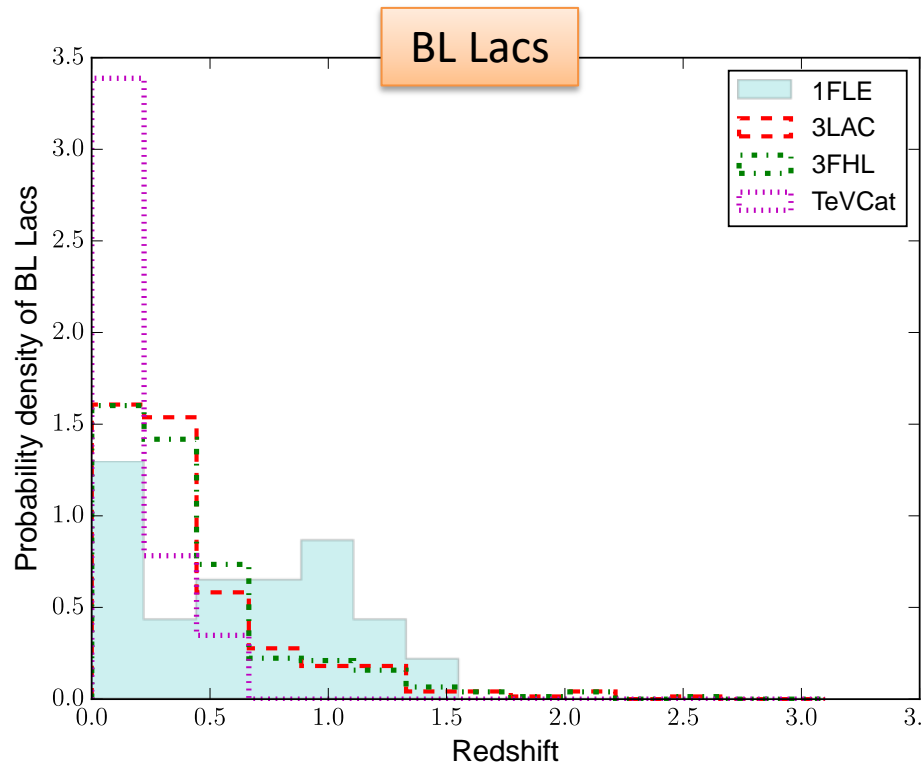
1FLE Blazars

Comparison of the blazars in 1FLE and in 3FGL(3LAC), 3FHL and TeVCat.

The higher fraction of FSRQs is expected in 1FLE since they typically have softer spectra than BL Lacs.



1FLE Blazars – Redshift distributions

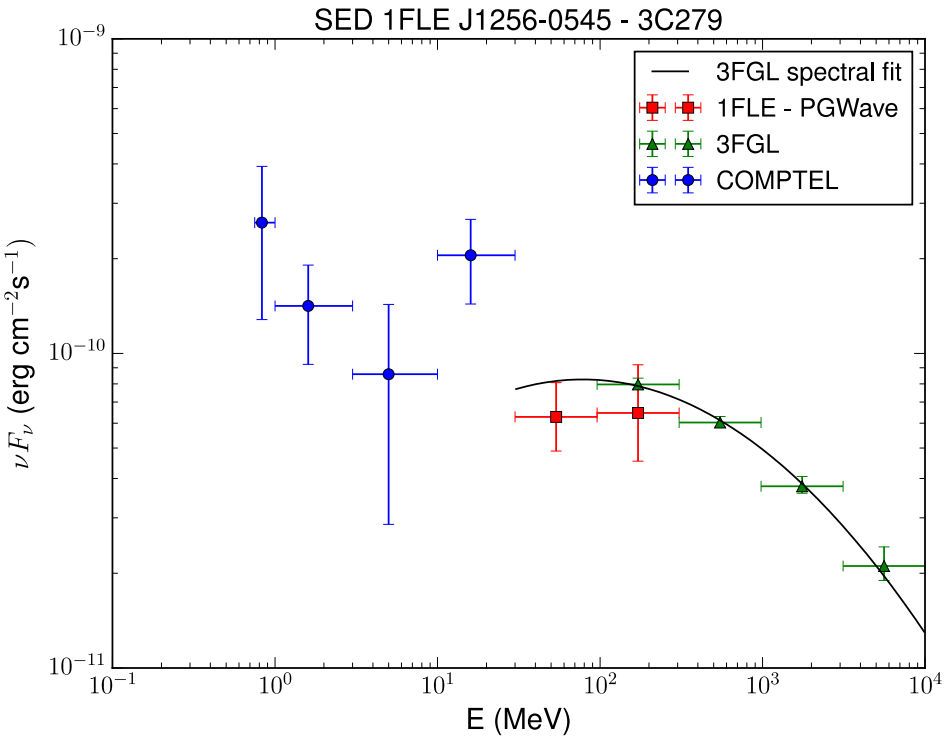
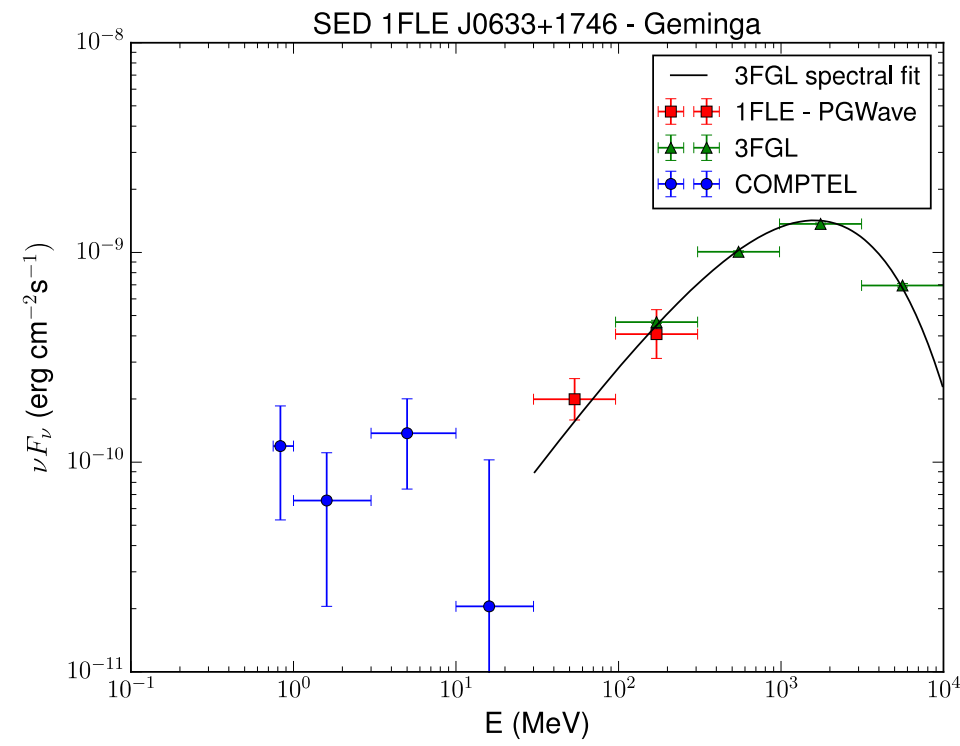


60% LSP BL Lacs in 1FLE,
compared to 25% in 3LAC.
LSP – Low-synchrotron
peaked blazar.

| Blazar class | 1FLE | 3LAC | KS test |
|---------------|-----------------|-----------------|----------------------|
| | z_{av} | z_{av} | p-value |
| All blazars | 1.06 ± 0.06 | 0.84 ± 0.02 | 8.1×10^{-6} |
| FSRQ | 1.22 ± 0.06 | 1.21 ± 0.03 | 0.964 |
| BL Lac | 0.59 ± 0.09 | 0.41 ± 0.02 | 0.018 |
| Other blazars | 0.55 ± 0.17 | 0.33 ± 0.04 | 0.124 |

Spectral Energy Distributions

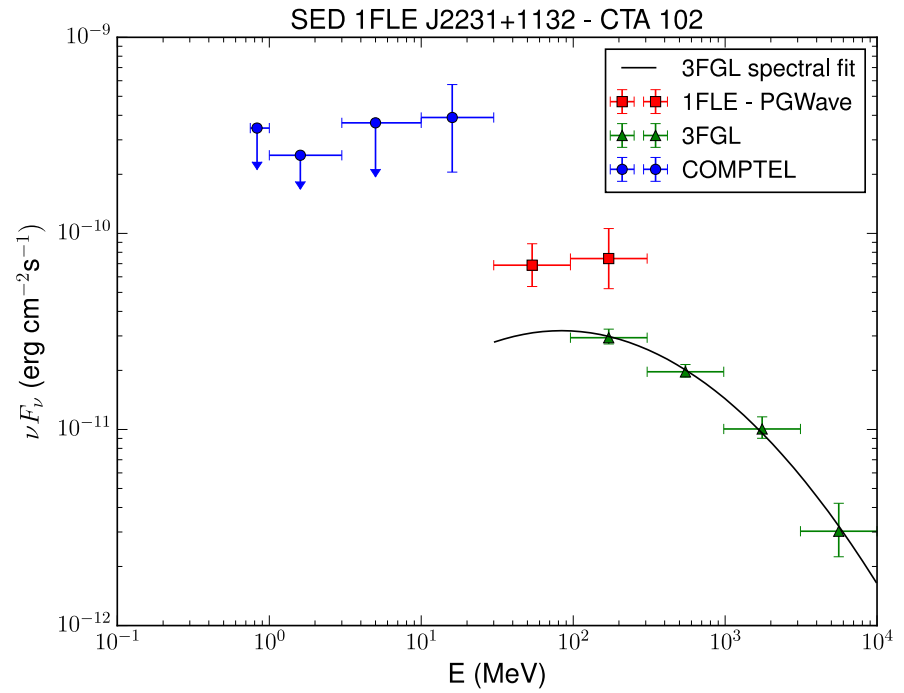
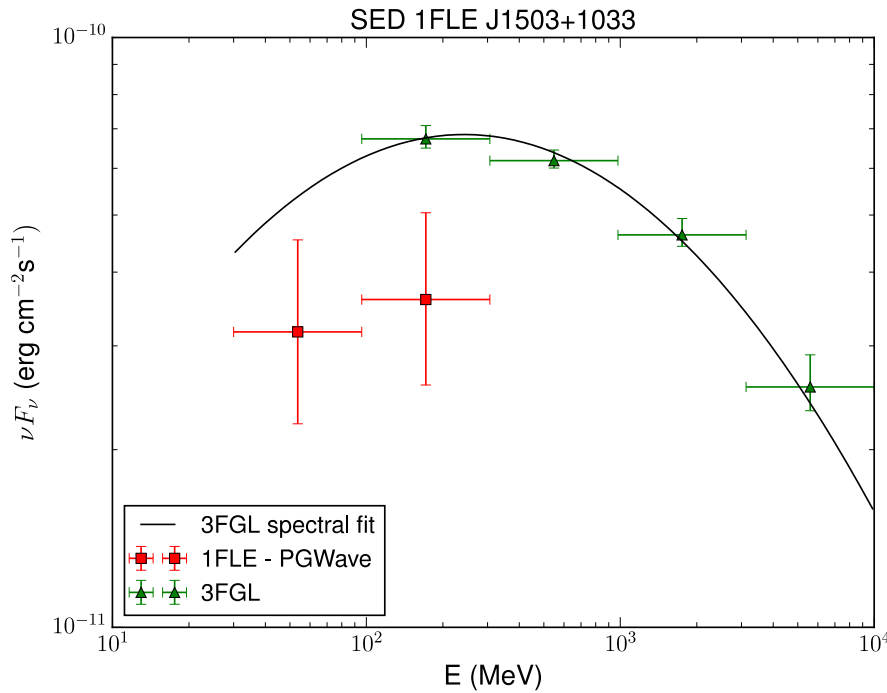
Two examples of SED.



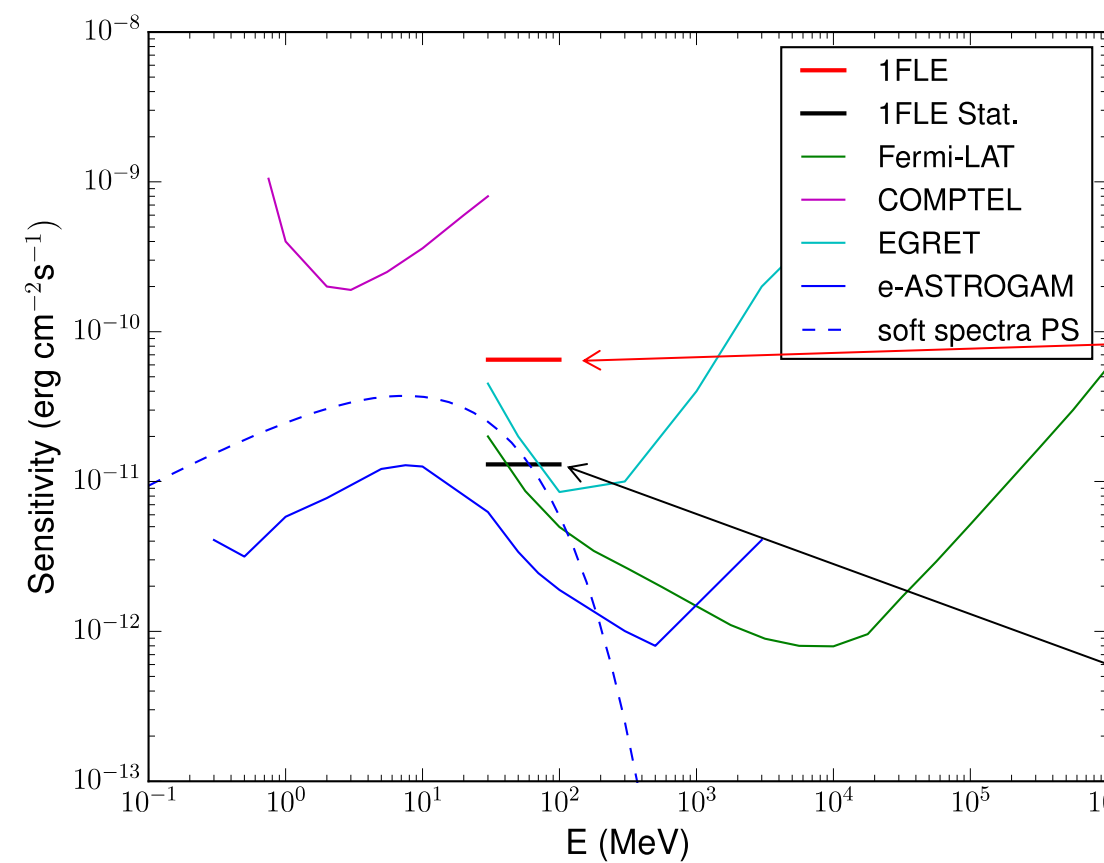
1FLE AGN flares

| Source Name | GLON (deg) | GLAT (deg) | 1FLE νF_ν (100-100 MeV) $10^{-12} \text{ erg cm}^{-2} \text{ s}^{-1}$ | 3FGL νF_ν (100-300 MeV) $10^{-12} \text{ erg cm}^{-2} \text{ s}^{-1}$ | Flare comment |
|-----------------|---------------|---------------|---|---|------------------|
| 1FLE J0424-0042 | 194.8 | -32.6 | 5.49 ± 2.19 | 18.79 ± 1.17 | flare in 3FGL |
| 1FLE J0443-0024 | 197.5 | -28.2 | 6.26 ± 2.50 | 19.72 ± 0.86 | flare in 3FGL |
| 1FLE J1224+2118 | 255.5 | 81.6 | 49.77 ± 14.79 | 83.52 ± 1.12 | flare in 3FGL |
| 1FLE J1227+0218 | 289.1 | 64.6 | 37.46 ± 10.63 | 87.53 ± 1.41 | flare in 3FGL |
| 1FLE J1332-0518 | 321.6 | 56.0 | 11.93 ± 3.39 | 26.22 ± 1.93 | flare in 3FGL |
| 1FLE J1503+1033 | 11.3 | 54.8 | 3.60 ± 1.02 | 6.73 ± 1.19 | flare in 3FGL |
| 1FLE J2231+1132 | 77.1 | -38.6 | 74.32 ± 22.09 | 29.34 ± 1.03 | flare after 3FGL |

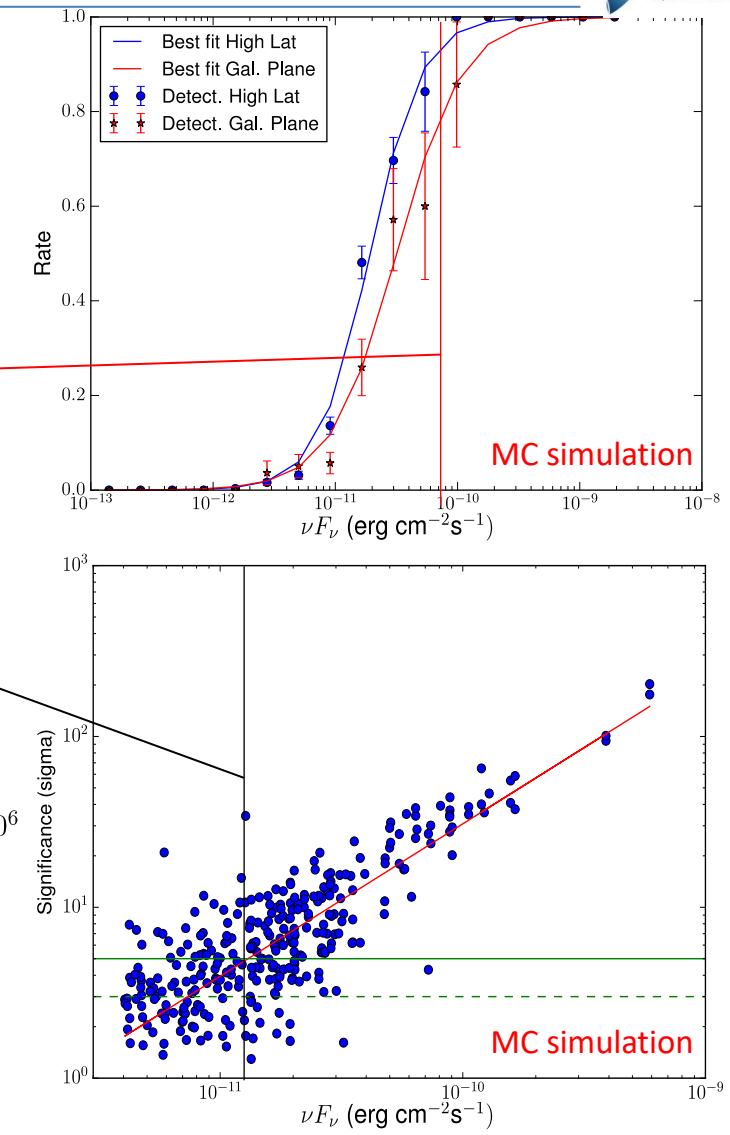
Table 5. 1FLE sources with a flare during the 3FGL observation time (flare in 3FGL) or after the 3FGL observation time (flare after 3FGL).



1FLE Sensitivity



In red, the **1FLE total sensitivity** (95% detection efficiency at $|b| > 10^\circ$), while in black the **1FLE statistical sensitivity** determined as the flux corresponding to the 5σ significance of PGWave.



Summary

Simulation:

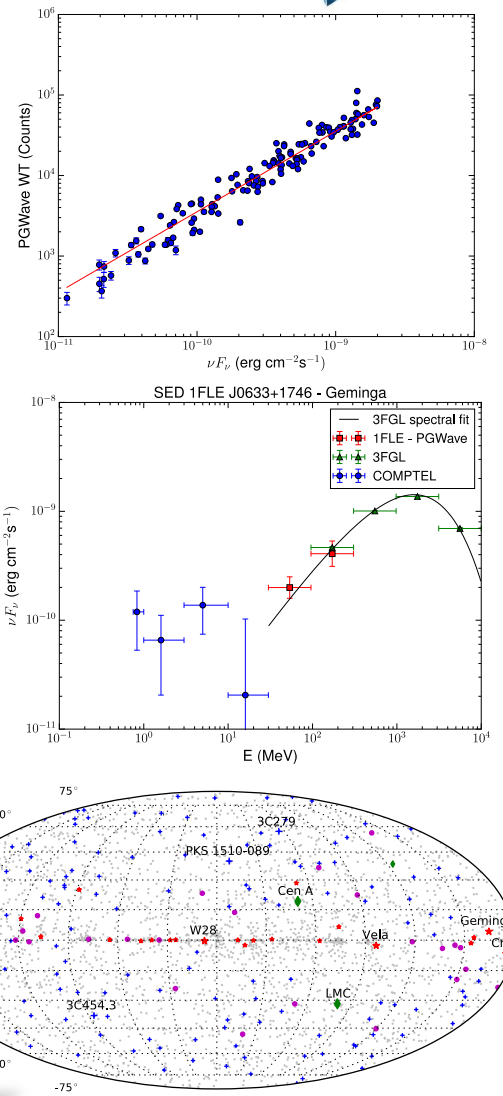
1. We optimize the PGWave parameters to maximize detection rate and minimize the false positives.
2. We optimize the reconstructed position with a parabolic fit.
3. Using 10 realization maps, we estimate the Stat. and Syst. Unc. Source Localization.
4. Flux Reconstruction:
 - We reconstruct the flux using the WT peak
 - We estimate the Stat. and Syst. Unc. for flux reconstruction

Results:

1. We analyze 8.7 years of data between 30-100 MeV: we found 198 PS, 187 have an association in 3FGL and 11 have no association (no significant evidence of new sources).
2. We compare the 1FLE AGNs with other gamma ray catalogs (3LAC, 3FHL, TeVCat).
3. We create the spectral energy distributions for the 1FLE PS.
4. We estimate the sensitivity of the 1FLE catalog.

Recently accepted by A&A and posted on arXiv

Thanks for your attention



Backup Slides

PGWave: a Wavelet Transform Method

PGWave is a method, based on **Wavelet Transforms** (WTs) [1], to detect sources in astronomical images obtained with photon-counting detectors, such as X-ray or gamma-ray images.

1. The WT of a 2-dim image $f(x,y)$ is defined as:

$$w(x, y, a) = \iint g\left(\frac{x - x'}{a}, \frac{y - y'}{a}\right) f(x', y') dx' dy'$$

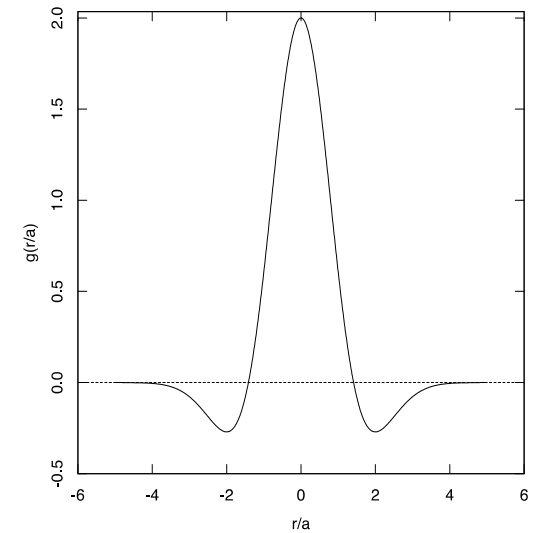
where $g(x/a, y/a)$ is the generating wavelet, x and y are the pixel coordinates, and a is the scale parameter.

2. PGWave uses the 2-dim “**Mexican Hat**” wavelet:

$$g\left(\frac{x}{a}, \frac{y}{a}\right) \equiv g\left(\frac{r}{a}\right) = \left(2 - \frac{r^2}{a^2}\right) e^{-r^2/2a^2} \quad (r^2 = x^2 + y^2)$$

3. The peak of the WT for a source with Gaussian shape (N_{src} total counts and width σ_{src}) is:

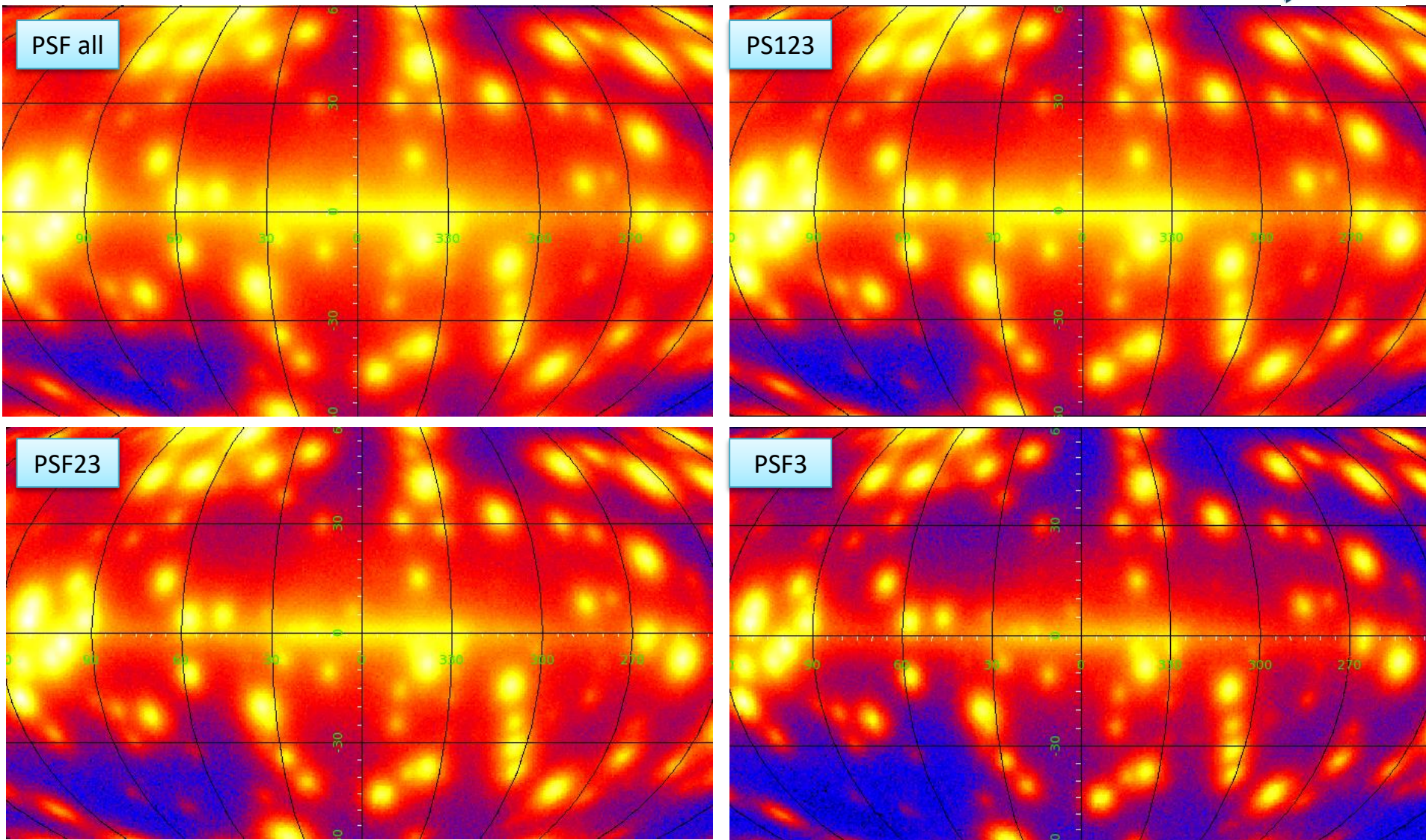
$$w_{peak}(a) = \frac{2N_{src}}{(1 + \sigma_{src}^2/a^2)^2}$$



[1] Damiani F. et. al., A Method Based on Wavelet Transforms for Source Detection in Photon-Counting Detector Images, ApJ 483, 350, (1997)

PSF Class Selection

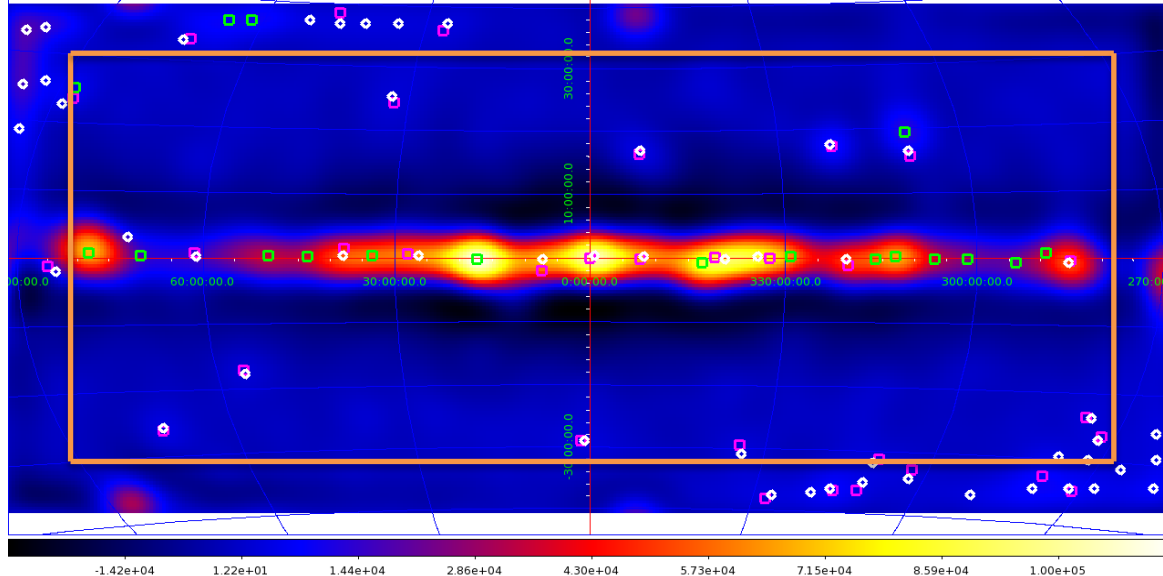
Random PS maps



Analysis Procedure

Analysis procedure:

1. Gtbin: we use 12 ROIs of the dimensions of $180^\circ \times 90^\circ$ (LON, LAT)
2. PGWave: we perform PGWave and create a dictionary
3. Restrict area: we eliminate the seeds that are close to the boarder
4. Merge seeds: we merge the seeds in the overlapped regions
(we perform the previous steps 1-4 are performed also for the diffuse maps)
5. Eliminate diffuse: we eliminate the seeds that match with those from the diffuse
6. Comparison: we compare the resulting sources with the 3FGL
7. Flux determination: we determine the flux using the WT peak of PGWave

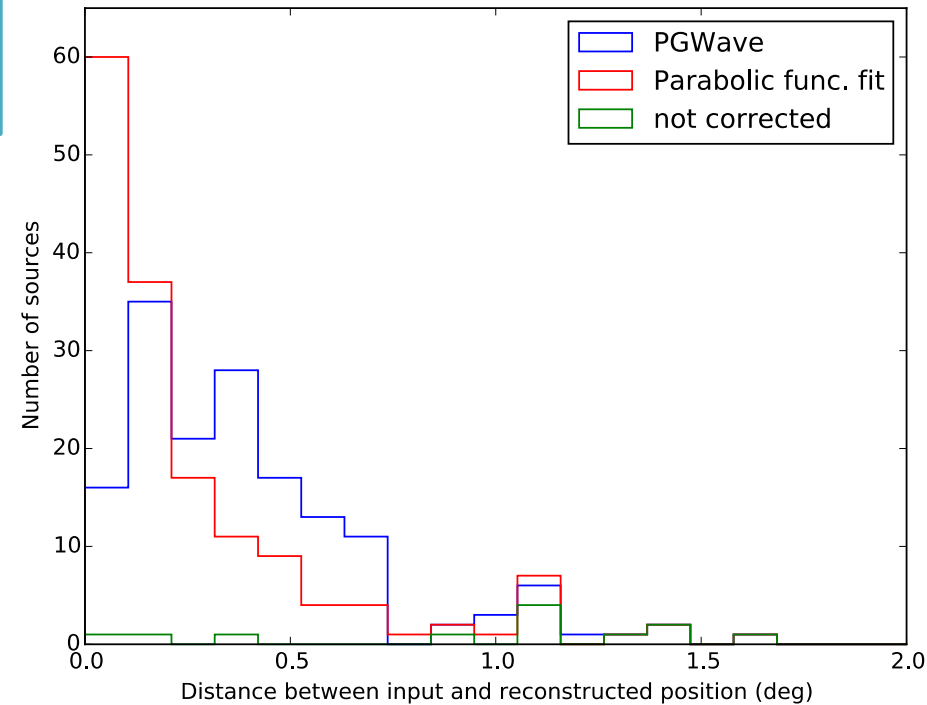
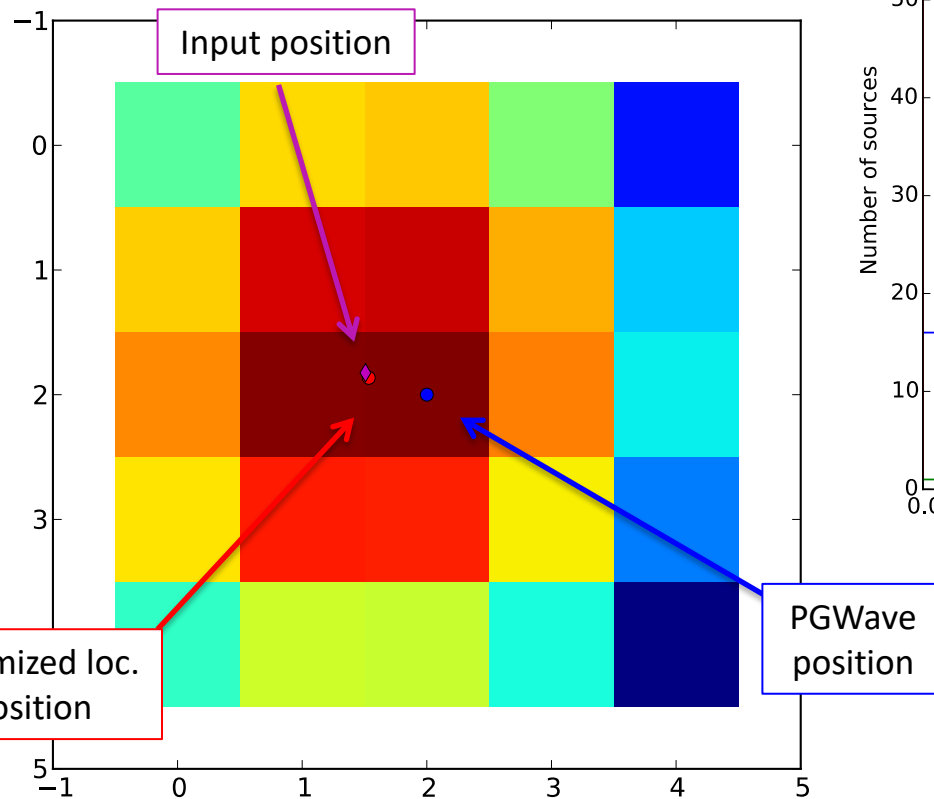


Data Selection

| Data Selection | Values |
|----------------|----------------------------|
| IRFs | P8R2_SOURCE_v6 |
| PSF Classes | PSF3 |
| Time Interval | 8.7 years |
| Energy Range | [30-100 MeV] [100-300 MeV] |
| Zenith angle | 90° |
| Pixel Size | 0.458° |

Optimized localization

Since PGWave returns the positions of the center of the pixel (in which the WT has a maximum), we optimize the reconstruction of the position using a parabolic fit in 5x5 pixel grid around the maximum.



Tolerance radius (1°.5): 98% of the reconstructed sources are localized at less than 1°.5 from the input position.

We used 10 realizations of the MC maps with random positioned PS for studying the systematical and statistical error in the localization ([30-100 MeV], {100-300 MeV}].

Statistical:

for each reconstructed PS (K) we compute the mean and the standard deviation (sigma) of the position of the seeds from the different realizations, with the mean position X_{mean}

$$\sigma = \sqrt{\frac{\sum(X_{PGW_i} - X_{PGWmean})^2}{n}} \quad \sigma_k = \frac{\sigma}{\sqrt{n-1}}$$

where n is the number of PGWave seeds associated at this reconstructed PS (input PS). Our statistical Unc. is the mean of all the single σ_k of each reconstructed PS

$$\sigma_{stat} = \sqrt{\frac{\sum_k \sigma_k^2}{k}}$$

Total Deviation in the Position (Systematic)

We compute the difference between the mean position for the seeds of the same reconstructed PS and the position of the input PS:

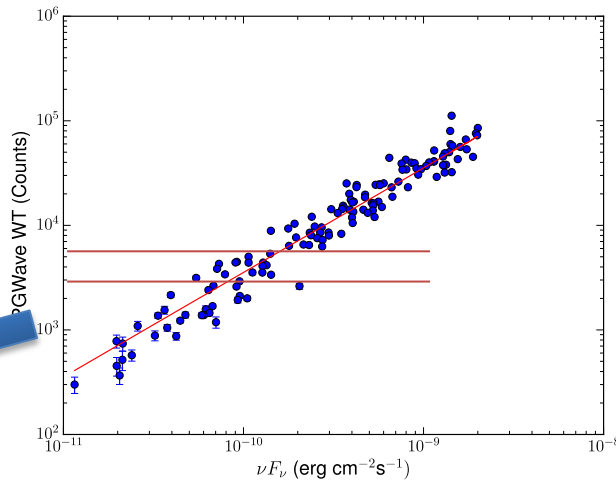
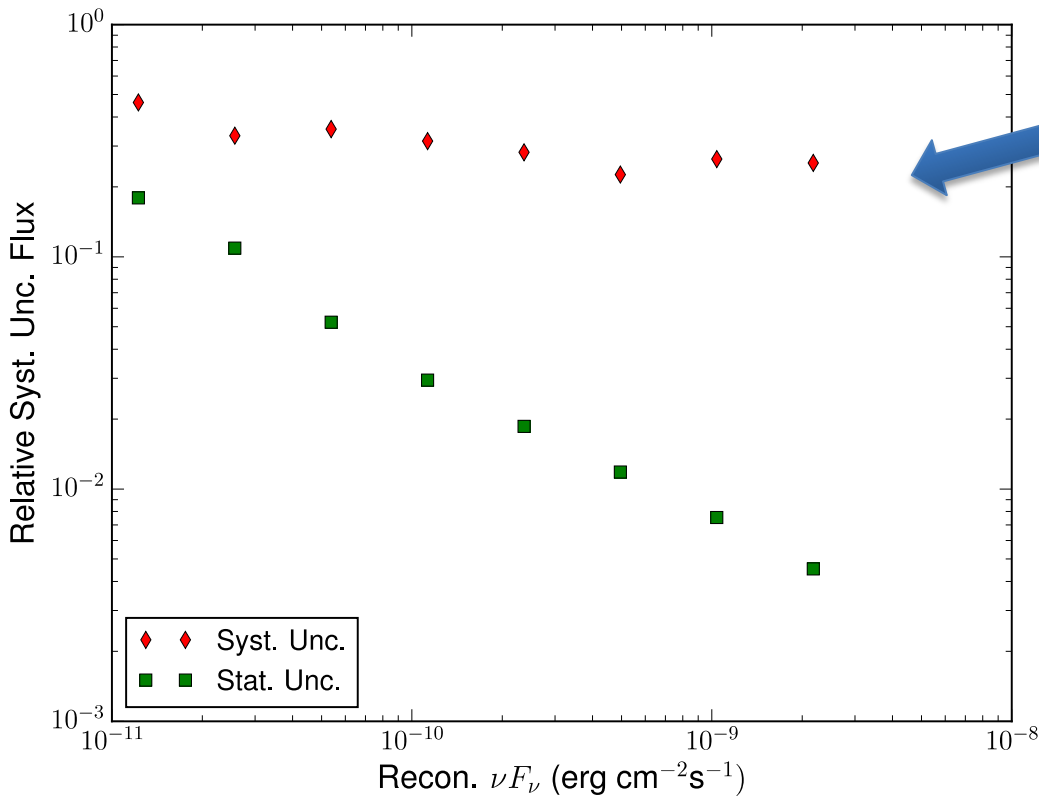
$$\Delta_k = X_{PGWmean} - X_{IN}$$

Then for all the reconstructed PS

$$\sigma_{DEV} = \sqrt{\frac{\sum \Delta_k^2}{k}}$$

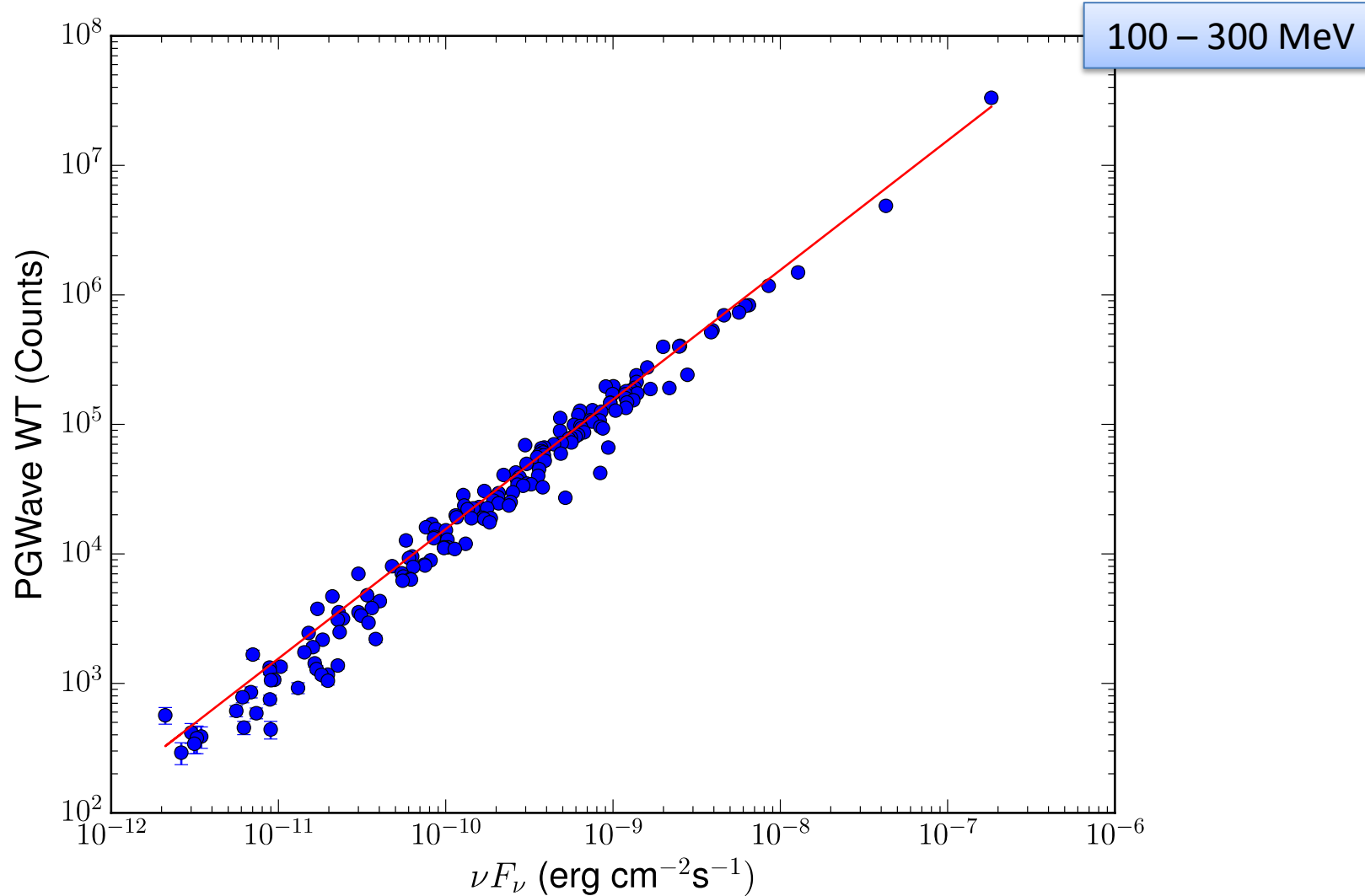
Stat. and Syst. Unc. of Flux Reconstruction

To derive the Syst. Unc. of the Flux Reconstruction, we divide the sources in bins of WT peak, then we estimate the mean distance, inside each bin, between the Input MC Flux and the PGWave best fit. (Stat. Unc. given by PGWave)



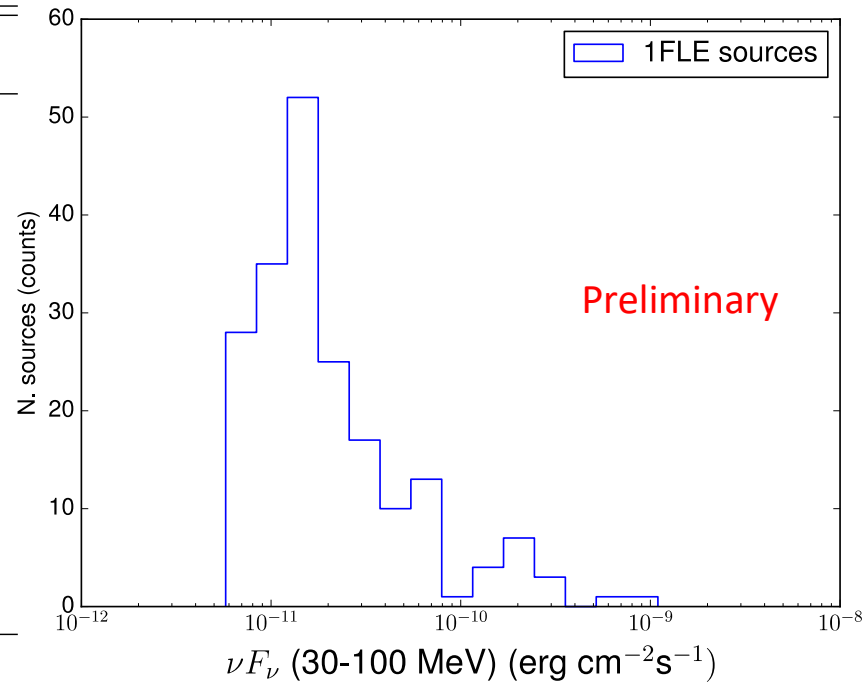
Relative Stat. and Syst. Unc
of Flux estimation
30 – 100 MeV

Flux Determination



1FLE sources characteristics

| Description | Associated Designator | Number |
|---|-----------------------|--------|
| Pulsar | psr | 12 |
| Pulsar wind nebula | pwn | 2 |
| Supernova remnant | snr | 2 |
| Supernova remnant / Pulsar wind nebula | spp | 5 |
| High mass binary | hmb | 1 |
| BL Lac type of blazar | bll | 31 |
| Flat spectrum radio quasar type of blazar | fsrq | 98 |
| Narrow-line seyfert 1 | nlsy1 | 1 |
| Radio galaxy | rdg | 3 |
| Steep spectrum radio quasar | ssrq | 1 |
| Normal galaxy (or part) | gal | 1 |
| Blazar candidate of uncertain type | bcu | 13 |
| Unclassified | " | 17 |
| Unassociated | - | 11 |
| Total in the 1FLE | | 198 |



Source classes of the 1FLE sources determined using the 3FGL associations.

Little evidence that the 11 sources with no 3FGL association are actually new sources.

1FLE sources not associated to the 3FGL

| Source Name | GLON (deg) | GLAT (deg) | Err_pos (deg) | Signif. (σ) | $\int F_{\nu} (30 - 100 M eV) 10^{-12} \text{ erg cm}^{-2} \text{ s}^{-1}$ | $\int F_{\nu} (100-300 \text{ MeV}) 10^{-12} \text{ erg cm}^{-2} \text{ s}^{-1}$ | Comment |
|-----------------|---------------|---------------|------------------|-------------------------|--|--|--------------|
| 1FLE J2206+7040 | 110.02 | 12.06 | 0.25 | 4.38 | 23.75 ± 7.16 | 0.0 ± 0.0 | Diffuse |
| 1FLE J0330+3304 | 157.42 | -18.94 | 0.25 | 9.87 | 23.56 ± 7.10 | 0.0 ± 0.0 | 3FGL sources |
| 1FLE J0422+5243 | 151.75 | 2.07 | 0.25 | 7.00 | 22.73 ± 6.85 | 0.0 ± 0.0 | Gal. plane |
| 1FLE J0647-0345 | 215.89 | -2.48 | 0.25 | 7.75 | 17.71 ± 5.34 | 0.0 ± 0.0 | Gal. plane |
| 1FLE J0655-1106 | 223.33 | -4.08 | 0.25 | 4.01 | 14.93 ± 4.94 | 4.07 ± 1.63 | Gal. plane |
| 1FLE J0522+3734 | 170.17 | 0.68 | 0.25 | 5.00 | 13.66 ± 4.52 | 0.0 ± 0.0 | Gal. plane |
| 1FLE J0637-0110 | 212.35 | -3.72 | 0.25 | 4.80 | 10.88 ± 3.6 | 0.0 ± 0.0 | Gal. plane |
| 1FLE J1033+1601 | 224.87 | 56.14 | 0.25 | 3.65 | 10.30 ± 3.41 | 0.0 ± 0.0 | $\sigma < 4$ |
| 1FLE J2158-5424 | 339.89 | -48.37 | 0.25 | 3.99 | 8.51 ± 2.82 | 0.0 ± 0.0 | $\sigma < 4$ |
| 1FLE J1203-2504 | 289.40 | 36.53 | 0.25 | 4.07 | 8.39 ± 2.77 | 0.0 ± 0.0 | 3FGL sources |
| 1FLE J1030-3133 | 270.81 | 22.38 | 0.25 | 3.43 | 7.11 ± 2.35 | 0.0 ± 0.0 | $\sigma < 4$ |

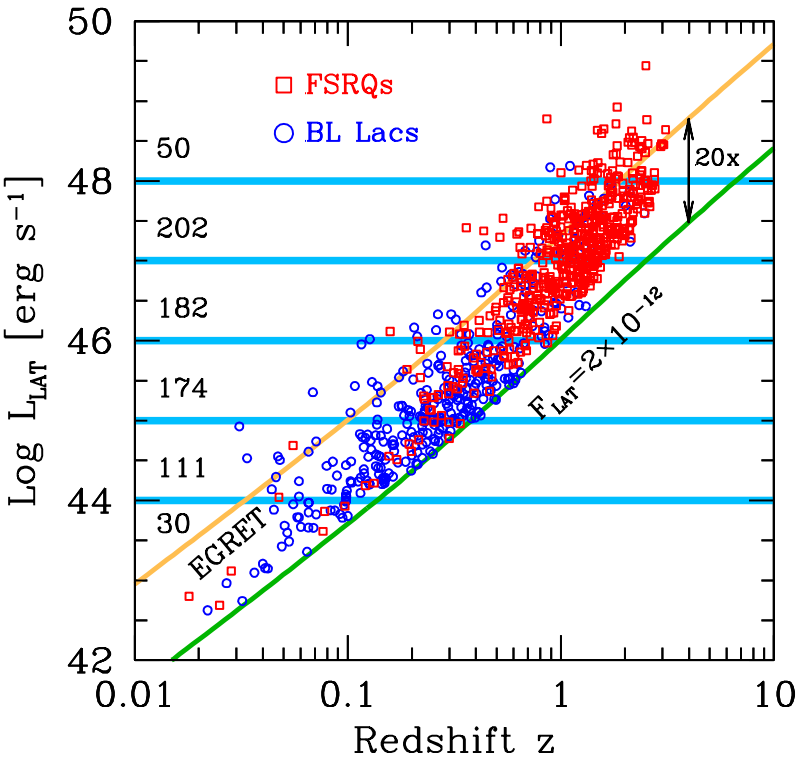
Gal. Plane: inside the galactic plane $|b| < 10^\circ$ where the diffuse emission has several structures.

Diffuse: particular regions where the diffuse emission has some bright features.

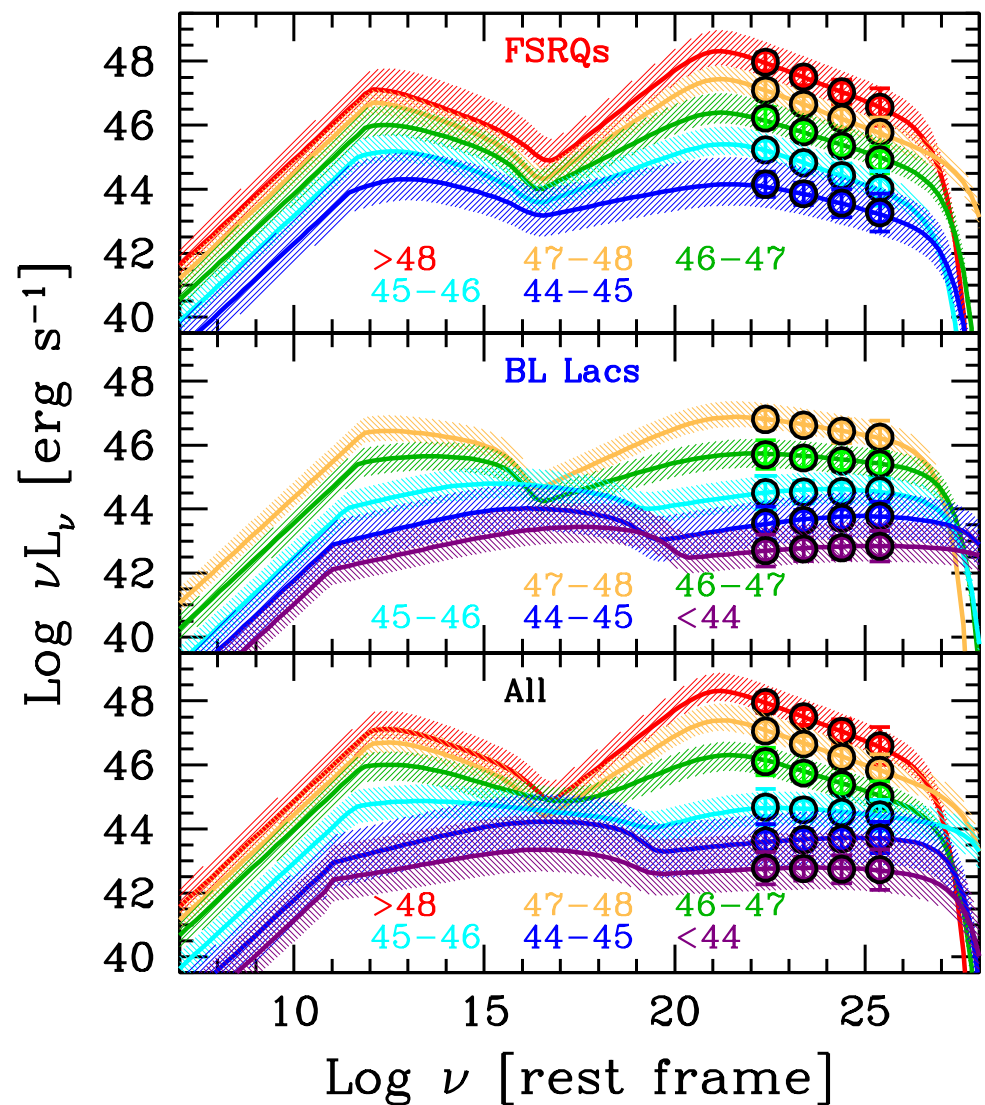
3FGL sources: due to the large PSF if there are two or more 3FGL sources close each other, they could form a single structure and PGWave does not distinguish the different sources but returns a seed in the middle.

Fermi blazar sequence

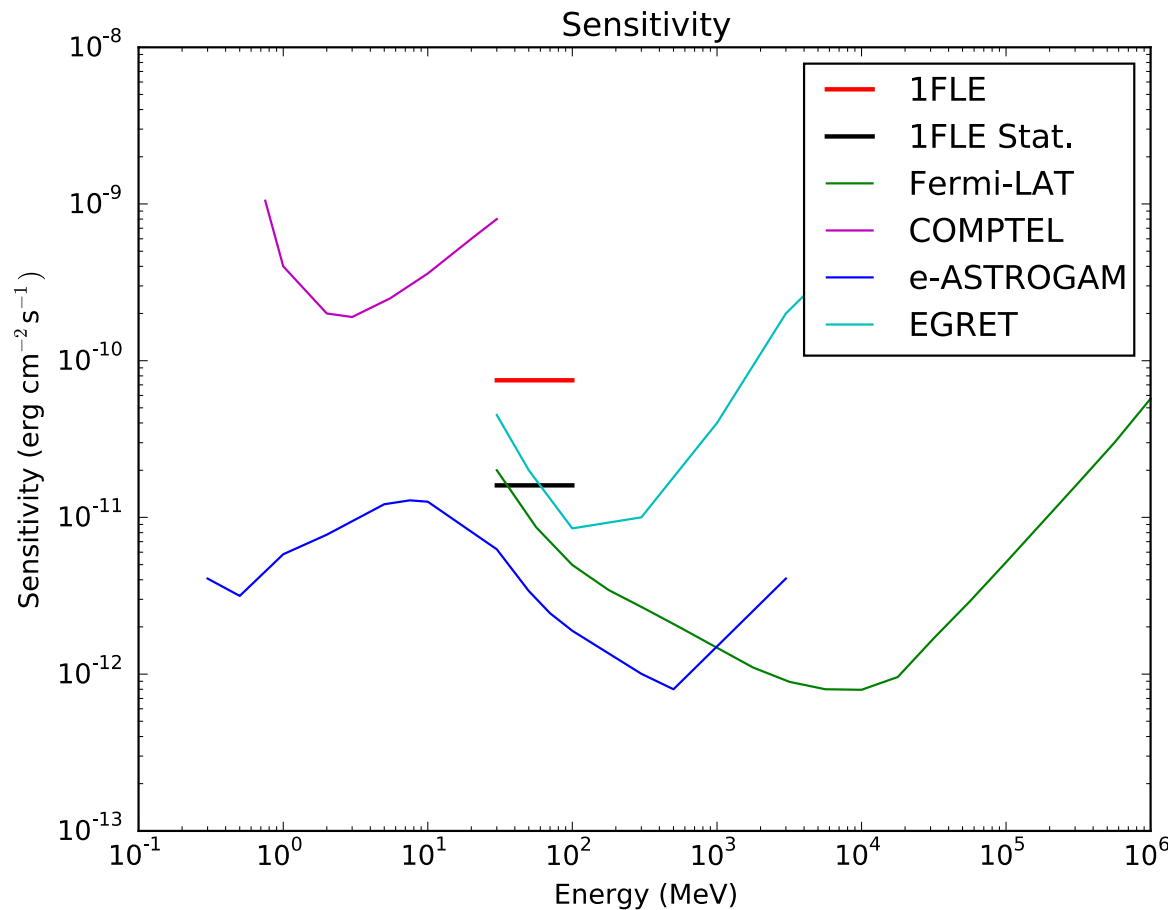
Using the 3LAC blazars



Ghisellini *et. al.* 2017



1FLE Sensitivity

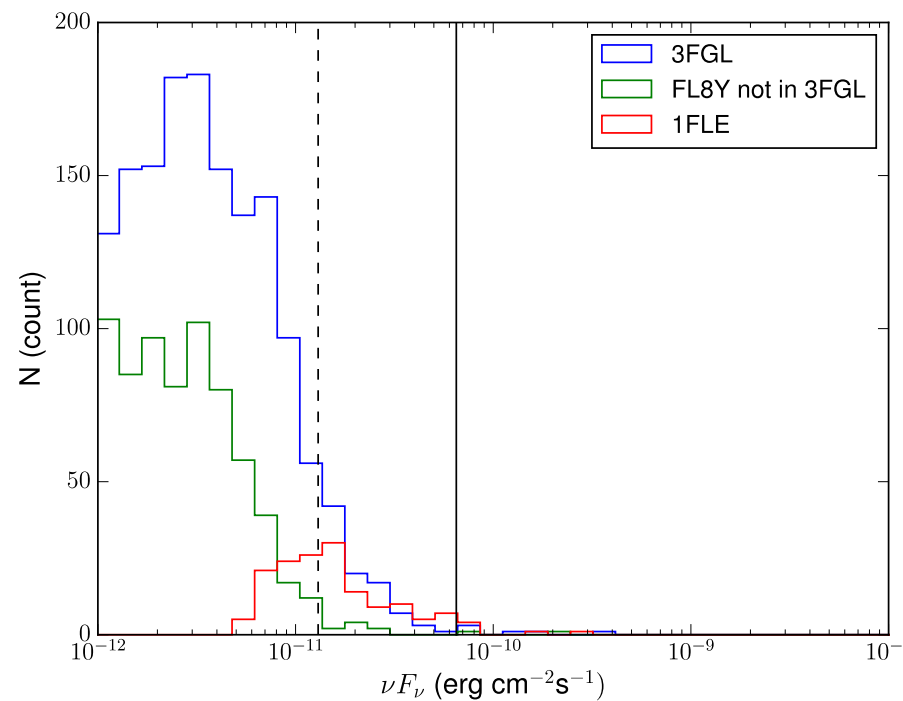


The **COMPTEL** and **EGRET** sensitivities are given for the typical observation time accumulated during 9 years. The **Fermi-LAT** sensitivity is for a high Galactic latitude source in 10 years of observation in survey mode. **e-ASTROGAM** sensitivity for an effective exposure of 1 year and for a source at high Galactic latitude.

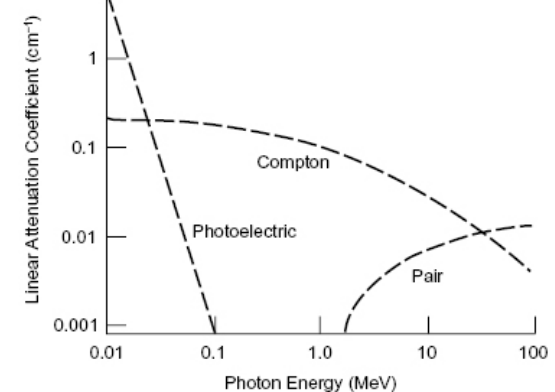
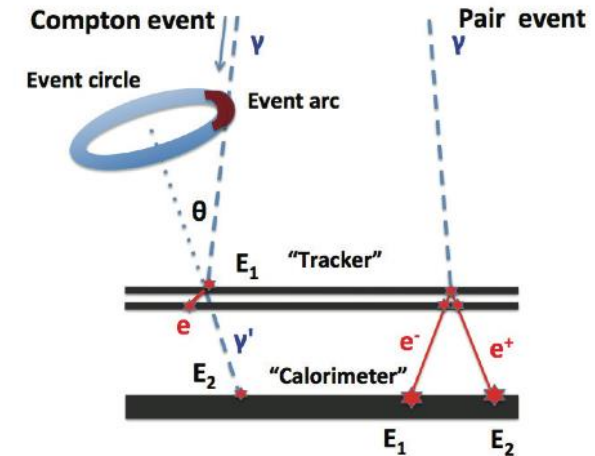
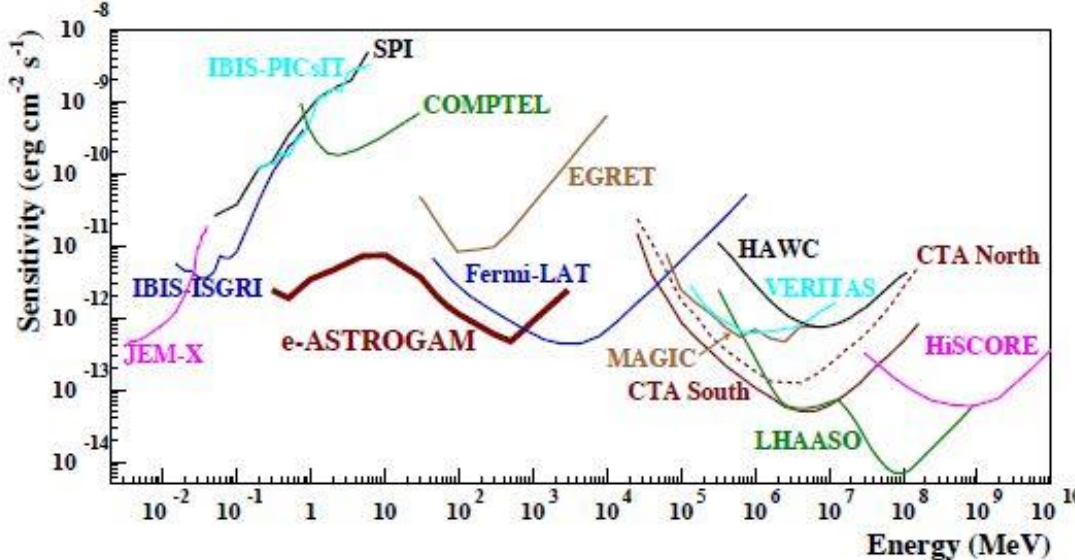
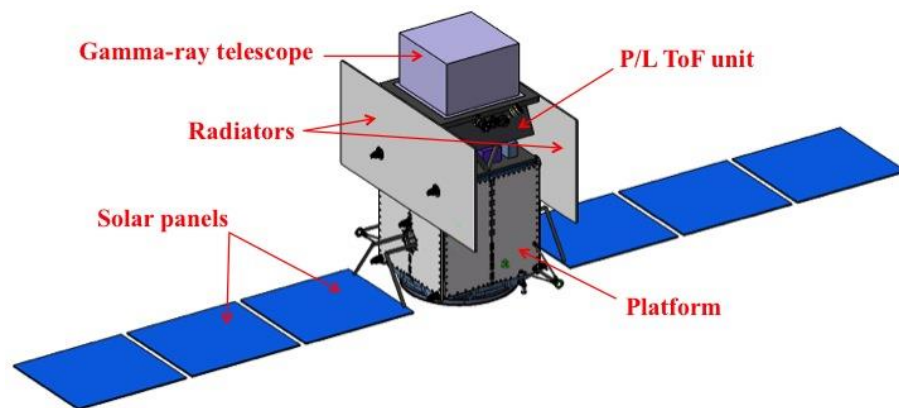
One of the reason of no new sources is the lower sensitivity of the Fermi-LAT at Low energies due to small effective area and angular resolution.

Two consequences of non-observation of new sources in 1FLE:

1. No sufficiently bright flaring sources (not in 3FGL) after 3FGL time interval
2. No very bright sources with a very soft spectrum, e.g. cutoff around 100 MeV



Outlook – eASTROGAM



De Angelis *et. al.* 2017